The Therapeutic Potential of Platelet- Rich Plasma and/or Mesenchymal Stem Cells on Diabetic Wound Healing: Histological and Immunohistochemical Study

Original Article

Badria Hassan Saad[1], Eman Elazab Beheiry[1], Nancy Mohamed El Sekily[1], Dina Mohamed Rostom[2], Samar S Ibrahim[3] and Rasha R. Salem[1]

[1]Department of Anatomy and Embryology, [2]Department of Histology and Cell Biology, [3]Center of Excellence for Research in Regenerative Medicine and Applications, Faculty of Medicine, Alexandria University, Egypt

ABSTRACT

Introduction: Non-healing wounds are a significant public health issue and a significant financial drain on the healthcare system. Platelet-rich plasma (PRP) was proved to be successful in numerous experiments as it is rich in many cytokines and proteins important for wound healing. Bone marrow- derived mesenchymal stem cells (BM-MSCs) release trophic factors that control inflammation and remodelling, thus it can aid in wound healing.

Objective: The aim of this study was to assess morphological, histological and immunohistochemical effects of PRP and/or BM-MSCs on cutaneous wound healing in diabetic rats.

Materials and Methods: Hundred healthy male albino rats; ten rats were used as mesenchymal stem cells and PRP donors. Eighteen rats were used as negative control group (A). Seventy-two rats (B) were divided into 4 groups 18 rats each after induction of diabetes by streptozotocin (STZ) drug and formation of skin wounds; Group I: positive control group, Group II: received single dose of PRP injection in the wound, Group III: received single dose of BM-MSCs injection in the wound, Group IV: BM-MSCs plus PRP. Cutaneous wounds were inspected and photographed every 2 days of the study period for morphological study. Six rats from each group were operated upon on days 7, 14, 30 of the study for histological and immunohistochemical studies.

Results: The best healing results were seen in group IV regarding morphological, histological and immunohistochemial results with a statistically significant difference between group IV and other study groups. Group III showed better healing results than in group II which was better than that of group I.

Conclusion: There is a synergistic effect of combined BM-MSCs and PRP on healing of skin wounds in STZ-induced diabetic rats which is better than to use either of them alone.

Received: 18 March 2024, **Accepted:** 26 April 2024

Key Words: Bone marrow derived mesenchymal stem cells, cutaneous wounds, diabetes, platelets rich plasma.

Corresponding Author: Badria Hassan Saad, PhD, Department of Anatomy and Embryology, Faculty of Medicine, Alexandria University, Egypt, **Tel.**: +20 12 8565 4211, **E-mail:** bedor_hefny@yahoo.com

ISSN: 1110-0559, Vol. 48, No. 2

INTRODUCTION

In vertebrates, the skin is the most substantial organ, it covers the whole surface area of the body and represents about 15% to 20% of body mass[1]. The skin is a substantial, complex immunological organ that regulates body temperature, performs a variety of sensory functions, and protects the host. It is very important in the defence against infections and in allergic responses[2]. The skin is formed of two crucial layers which are epidermis and dermis[3]. There are many types of cells in the dermis. The fibroblast is the main cell in dermis, it is responsible for producing extracellular matrix material, elastic and reticular fibres, and collagen. Inflammatory mast cells are located in dermal perivascular regions. These cells secrete vasoactive and proinflammatory mediators which play a necessary role in inflammatory responses, collagen remodelling, and wound healing[4].

A wound is a disruption of the skin's natural anatomical structure and functional integrity[5]. Wounds that remain unhealed are a significant public health issue and a significant financial drain on the healthcare system. They are present in a variety of illnesses, including cancer, burns, trauma, venous and pressure ulcers, diabetes mellitus and ischemia[6]. Serious problems including amputation in cases of diabetic foot ulcers (DFUs), scarring and deformity from burns, and life- threatening functional disability are all related to non-healing wounds[7]. Cancer development is also linked to non-healing wounds, particularly squamous cell carcinoma, most likely as a result of repeated tissue injury and accelerated cell growth[8].

Around 415 million people globally have diabetes, which is now the third most dangerous chronic illness affecting the health of humans[9,10]. Each year, 2 % of diabetic individuals get foot ulcers, and from 14 to 24%

DOI: 10.21608/ejh.2024.276171.2040

of them require amputation[9]. Actually, the typical healing process is messed up in wounds of diabetics because there aren't enough growth hormones, there's too much inflammation, and there aren't enough cells that normally repair damage. Consequently, the urgent problem of diabetic wound healing has emerged[9].

Haemostasis / inflammation, angiogenesis / cell proliferation, and remodelling are the three or four overlapping phases of the process of healing wounds that are controlled by different cells, cytokines, and growth factors[7,11].

Numerous studies have focused on creating better tools and methods in order to speed up diabetic patients' wound healing process. However, treating DFUs is still difficult for doctors, and many patients end up needing amputations[12,13]. Recently, regenerative methods for treating DFUs have included growth factors, different cell-based treatments, and platelet-rich plasma (PRP)[14,15]. Stem cells of mesenchymal type (MSCs) or PRP have been studied extensively for promoting the renewal of a variety of tissues, as the skin[15].

Growth factors (GFs), particularly PRP, have received a great deal of interest since the 1990s because they can preserve normal tissue structure and heal tissue damage[16]. PRP is a naturally occurring medical technology, its ability to promote and enhance tissue regeneration was the cause to attract interest in the field of regenerative medicine[1].

To recover from diabetic wounds, researchers have been looking at the use of PRP. It has been proved to be successful in numerous animal and clinical experiments because it is rich in several cytokines and proteins necessary for wound healing[9].

The MSCs are one type of stem cells which is now the subject of extensive research. Some tissues have been effectively treated and regenerated using stem cell-based therapies, and it has been demonstrated that MSCs have a variety of therapeutic applications. These stem cells have the capacity for differentiation into a wide variety of cells[17]. Moreover, they have the capacity to release specific cytokines and many growth factors that promote the healing process at injury sites[17,18].

Bone marrow- derived mesenchymal stem cells (BM-MSCs) can develop into many types of cells, as osteoblasts, adipocytes, myoblasts and neuronal cells, as well as epithelial cells of skin, lung, liver, kidney, and the digestive tract[19,20]. By releasing various trophic factors regulating regeneration and inflammatory processes, BM-MSCs can aid in wound healing[21].

The purpose of this study is to assess the possible morphological, histological and immunohistochemical effects of PRP and/or BM-MSCs on cutaneous wound repair in a model of induced diabetes in rats.

MATERIALS AND METHODS

Materials

Compounds

1. Streptozotocin (STZ): From Sigma Aldrich Company, U.S.A.
2. Polyurethane dressing (Tegaderm film): From Alex Company for Medical Equipment.
3. Platelet-rich plasma (PRP): was prepared in the laboratory of biochemistry department (El Mowasah), Faculty of medicine, Alexandria University, Alexandria, Egypt.
4. Bone marrow-derived mesenchymal stem cells (BM-MSCs): It was extracted in center of excellence in research for regenerative medicine and its applications (CERMA), Faculty of medicine, Alexandria University, Alexandria, Egypt.

Experimental Animals

This study was done on 100 healthy male albino rats. Ninety-five of which were adults at an age of six weeks and had a weight ranged from 200 to 250 g. The other five rats were at an age of two weeks and their average weight is 30 g and they were used for preparation of MSCs. The rats were from Animal House Center of Physiology Department (El Mowasah), Faculty of Medicine, Alexandria University. The rats were put in stainless steel cages under certain conditions as follows: 12 h dark/light cycle with temperature 22±2º C and humidity 50±10%, food and water were given ad libitum.

The rats were divided into:

1. Donor group (ten rats)
    - Five rats to prepare MSCs.
    - Five rats to obtain PRP.
2. Experimental study groups (ninety rats)
    - A (negative control group): 18 healthy non diabetic non injured rats.
    - B (diabetic study groups): 72 rats

The rats were divided by random into four study groups and each group included 18 rats as follows:

Group I (positive control group): the wound was dressed daily by normal saline and application of polyurethane dressing[22].

Group II (PRP group): Single dose of 1 ml PRP was injected in wounds at the first day of the study (day 0) and then application of the polyurethane dressing was done[19,23].

Group III (BM-MSCs group): Single dose of 1ml (3x106 cells/ml) of BM-MSCs was injected into the wounds at the first day of the study (day 0) and then application of the polyurethane dressing was done[23].

Group IV (BM-MSCs plus PRP): Single dose of 1ml ($3x10^6$ cells/ml) of BM-MSCs plus single dose of 1 ml of PRP were injected into the wound at the first day of the study (day 0) and then application of the polyurethane dressing was done[19,23].

Methods

Preparation of BM-MSCs

Bone marrow- derived mesenchymal stem cells (BM-MSCs) were extracted by flushing the bone marrow of the femurs and tibias of the rats with complete culture medium (CCM) under aseptic conditions using a 26-gauge needle. The culture medium was made up of Dulbecco's modified eagle medium with 10% fetal bovine serum as well as 1% penicillin-streptomycin. Centrifuging the bone marrow was done for twenty minutes then the cells were isolated and resuspended in CCM and then put into T-25 culture flask and incubated in humidified carbon dioxide incubator with 5% CO_2 for formation of colonies. After reaching 80% confluency, the cells were washed with phosphate buffer saline (PBS) and trypsinization was performed using 0.25% trypsin. Then the cells were centrifugated and put back in the culture medium and placed in the incubator in T-75 culture flask. BM-MSCs at passage 3 were used in the present study[19,20,24,25].

Characterization of BM-MSCs

Characterization was done by the following methods of investigation:

Morphologic characterization of BM-MSCs by inverted phase contrast microscope Nikon TSM inverted phase contrast microscope combined with a DCM 510 digital camera was used to follow-up the cultured cells[20]. Cultures from passages 0, 1, 2, and 3 were photographed when they were almost semiconfluent (at 50%, 60%, 70% and 80% confluency) respectively.

Immunophenotyping of BM-MSCs using flow cytometry To verify the phenotypic of BM-MSCs, the cultured cells after third passage were characterized for CD44, CD73 and CD90 as surface markers that are linked with MSC. In addition, other surface markers CD45 and CD11b which are predicted to be absent. After isolating the cells using a 0.25% trypsin-EDTA solution, the cells were rinsed with PBS and incubated for 30 minutes in the dark with monoclonal PE-conjugated antibodies for CD44 and CD45, AlexFlour555-conjugated antibodies for CD73, as well as FITC-conjugated antibodies for CD90. After three PBS washes, the cells were placed in 500 µL of FACS buffer. The FACS flow cytometer, using Cell Quest software (Becton Dickinson, USA), was used to analyze the cells[20,26].

Preparation of PRP

The rats were anaesthetized, ventral midline incision was done and then rat dissection was performed till reaching the inferior vena cava. The whole venous blood was extracted from the rats' inferior vena cava by a syringe and transferred to test tubes containing 3.2% sodium citrate. Then the blood was spun in a centrifuge for 10 minutes at 400g. After that, the supernatant was put in another tube to be recentrifuged at 800g for 10 minutes followed by removing the upper 2/3 of plasma as it contains platelet poor plasma. The lower 1/3 was considered as PRP. PRP was isolated using a pipette technique[23,27].

Diabetic study groups

All rats were exposed to the following:

a. Induction of diabetes

In order to induce diabetes, STZ dissolved in sodium citrate at a dose of 40 mg/kg was injected once intraperitoneally[28]. Levels of glucose in blood were measured seven days after STZ injection with a glucometer by blood tail sampling, rats whose levels of glucose ≥300 mg/dl were regarded to be diabetic[19,22].

b. Development of skin wounds

After diabetes mellitus (DM) induction with two weeks, the rats were anesthetized; the skin on the dorsal aspect of the trunk was shaved. A circular full thickness incision and dissection of this circular skin area was done leaving a circular raw area of 2 cm diameter under aseptic technique[19]. Wounds were daily examined and dressed by polyurethane dressing. The day of formation of wound was regarded as day 0[22].

Wound healing assessment

The cutaneous wounds in all study groups were cleaned daily with saline and new polyurethane dressing was applied.

a. Morphological study

1- By inspection

The cutaneous wounds were inspected for any signs of inflammation as redness of skin, signs of infection as pus formation, scab formation and for scar formation. The Time of complete wound healing was reported.

2- By image analysis software

The wounds were photographed every 2 days by digital camera till the end of study period (30 days) and were compared to that of day 0. The photographs were analyzed by image analysis software (FIJI/ImageJ software (NIH, Bethesda, NJ)) regarding the surface area of the raw area[19,22].

Closure of the wound was assessed by quantifying the re epithelialization of the open wound as a percentage of the area of original wound, it was measured by the following equation:

1 – (Open wound surface area/original wound surfaces area) x100%[8,19].

Degree of re-epithelialization was rated on a scale from 0 to 4 as follows:

0: wound closure is 0%.

1: wound closure is more than 0% and less than or equal 30%.

2: wound closure is more than 30 % and less than or equal 60%.

3: wound closure is more than 60% and less than or equal 99%.

4: wound closure is 100%[29].

b. Histological study

On the 7th, 14th and 30th day of the study period, from each group six rats were selected randomly and anesthetized then removal of the whole wound with intact skin margin was performed[30]. Skin specimens were fixed in 10% formol saline, then prepared by standard method and placed in paraffin wax. Then the blocks were sectioned into 5-6 µ thick sections followed by staining with:

1. Hematoxylin and eosin (H&E) stain
2. Masson's trichrome stain to demonstrate collagen fibers.

Then, the slides were examined and photographed by the light microscope. From each group stained by Masson's trichrome, six random high-power fields (HPF) in each specimen were selected on 7th, 14th and 30th day of the study period and analyzed by the color threshold tool using NIH FIJI/ImageJ software to measure collagen percentage in each sample. Data were presented as mean ± SD[20].

c. Immunohistochemical analysis

After deparaffinization and rehydration in decreasing alcohol grades, to block the activity of endogenous peroxidase 4 µ thick paraffin-embedded sections were treated for 10 minutes with 3% hydrogen peroxide and then 1% bovine albumin for 1 hour. Primary anti-CD68 antibody (mouse monoclonal Ab, clone KiM6, diluted 1:100) as well as secondary antibody conjugated with horseradish peroxide (rabbit antimouse IgG, diluted 1: 100) were used after antigen retrieval. The sections were incubated overnight to observe macrophage infiltration. Lastly, slides were counterstained with hematoxylin. After that, light microscope with a digital camera was used for semiquantitative microscopic assessment of the macrophage infiltration. Six high-power fields at random (HPF) were assessed in each specimen to count macrophages that have infiltrated. Data were displayed as mean ± SD[19,20].

Statistical analysis

Data was fed to the computer, then version 20.0 of the IBM Statistical Package of Social Sciences (SPSS) software was used to analyze data. (Armonk, NY: IBM Corp.). In order to check the normal distribution of data, Shapiro-Wilk test was used. Numbers and percentages were used to describe the qualitative data. The terms range (minimum and maximum), mean, standard deviation, and median were used to describe quantitative data. *P values* lower than or equal 0.05 were considered as statistically significant. To compare between different groups for categorical variables Chi-square test was used. To compare between the studied groups for normally distributed quantitative variables F-test (ANOVA) was used and for pairwise comparisons Post Hoc test (Tukey) was used. Abnormally distributed quantitative variables were tested using Friedman test to compare between the studied groups and Post Hoc (Dunn's) was used for pairwise comparisons[31,32].

RESULTS

Characterization of BM-MSCs

By examination with inverted phase contrast microscope, it was demonstrated that primary cells were adherent fusiform or polygonal in shape having multiple small cytoplasmic projections. The cultures from passages 0, 1, 2, and 3 denoted that morphology of cells and their proliferative abilities were maintained in all passages in the present study (Figures 1 a,b,c,d respectively)

A flow cytometry analysis of the BM-MSCs from passage 3 detected that they were positive for typical CD44, CD 73 and CD 90 surface marker and negative for CD11 and hematopoietic CD45. FACS analysis demonstrated that 98.3%, 96.6% and 98% of the cultured BMSCs expressed CD44, CD73 and CD90 respectively (Figures 2 a,b,c respectively). Two percnt, 3% only of the cells expressed CD45 and CD11b respectively (Figures 2 c,d respectively).

Morphological results

By inspection

The size of the wound area decreased obviously with statistical significance in groups II, III, IV in comparison with group I. Best and earliest healing was seen in group IV then group III then group II. The last group to heal was group I (Figures 3a,b,c,d).

Cardinal signs of inflammation represented in redness of skin of the wound edges obviously appeared in group I (control group) and with a lesser extent in group II (PRP group). While group III (stem cells group) and group IV (PRP + stem cells group) showed the least cardinal signs of inflammation (Figure 3a).

Signs of infection appeared in group I, this was seen as pus secretion (Figure 3a). Scab formation was demonstrated in groups I, II, III (Figure 3a).

After complete healing on day 30, the skin wound healed with obvious scar formation in group I (Figure 4a) while group II showed less prominent scar formation (Figure 4b) whereas, groups III & IV showed well healed skin wounds with intact skin with no scar formation (Figures 4 c,d respectively).

Regarding mean time of complete healing, there was a difference with a statistical significance between the four studied groups and between control group and other study

groups ($p \leq 0.05$) as group IV was the first group to reach complete healing with mean time (18.50 ± 1.05), followed by group III with mean time (23.17 ± 1.17), then group II with mean time (25.50 ± 1.05), and lastly group I with mean time (28.67 ± 0.82) (Figure 4e).

By image analysis software

During the study period, the surface area (SA) of the induced skin wound decreased with a statistical significance in study groups II, III, IV in comparison with group I and also between the four study groups ($p \leq 0.05$) in most of the study days (Figures 3 b,c,d). The means of SAs of induced skin wounds have reached zero level in group I on day 30, in group II on day 28, in group III on day 26 and in group IV on day 20 (Figure 3d).

Throughout the period of research there was increase in the wound closure percentage with a statistical significance in study groups II, III and IV in comparison with group I and hence an improvement in the degree of re-epithelialization. By the end of the first week the mean of wound closure % increased significantly in group II and was (47.62% ± 7.52) re-epithelization grade: 2 compared to group I that was (29.50% ± 7.27) re-epithelization grade: 1 and increased significantly in group III (56.92% ± 7.37) re-epithelization grade: 2 relative to groups I&II, and in group IV (66.42% ± 6.99) re-epithelization grade: 3 compared to other studied groups (Figures 5 a,b). By the end of second week the mean of wound closure % increased significantly in group II and was (90.48% ± 2.25) re-epithelization grade : 3 relative to group I that was (75.06% ± 4.79) re-epithelization grade : 3, and increased significantly in group III (94.58% ± 1.49) re-epithelization grade: 3 compared to groups I&II, and in group IV (98.93% ± 0.70) re-epithelization grade: 3 compared to other studied groups (Figure 5 c,d). The mean of wound closure % has reached 100% re-epithelization grade: 4 on day 30 in group I, day 28 in group II, day 26 in group III and day 20 in group IV (Figures 5 e,f).

At the end of 1st week, groups III & IV were the first to reach grade III by 33.3% & 72.2% respectively (Figure 5b) (Table 1). By the end of 2nd week there was no significant difference between the studied groups, and they all reached grade III by 100% (Figure 5d, Table 2). During the 3rd week of the study (day 18), only group IV was the first to reach grade IV. 100% of the same group reached grade IV on day 20. 100% of groups I, II, and III reached grade IV on days 30, 28 and 26 of the research period respectively (Figure 5f, Table 3).

Histological results

Hematoxylin and eosin (H&E) stain

Histological sections of group A, at higher magnification, showed thick epidermis covered by keratin with well-organized keratinocytes lying on intact basement membrane. Abundant keratohyaline granules were detected in stratum granulosum layer (Figure 6a). At lower magnification, the sections showed thick epidermis covered by keratin covering the dermis. Blood vessels, abundant hair follicles and sebaceous glands were found in the dermis. Papillary layer showed abundant deposition of fine interlacing collagen fibers. The reticular layer has thick organized collagen bundles running in different directions (Figure 6b).

On day 7, Histological sections of group I; at higher magnification, the epidermis showed disorganized keratinocytes, wide intercellular spaces in the stratum basale. Vacuolated cytoplasm and pyknotic nuclei were detected in stratum spinosum and the stratum granulosum layer showed a few keratohyaline granules (Figure 7a). At lower magnification, the sections showed most of the wound surface is covered by a scab with absence of epidermis but intact basement membrane with thin epidermis only at the edge of the wound. Areas of large fluid filled spaces seen between epidermis and underlying dermis (Figure 8a). Massive granulation tissue is filling the wound bed. Massive inflammatory cell infiltration, congested blood vessels, as well as minimal deposition of fine collagen fibers with absence of skin appendages were demonstrated in wound area (Figures 7a, 8a). Group II showed wound surface covered by a thin layer of epidermal cells. Moreover, the epidermis is covered by exudation (Figures 7b, 8b). Areas of large fluid filled spaces seen between epidermis and underlying dermis (Figure 7b). At higher magnification, the epidermis showed disorganized keratinocytes lying on an intact basement membrane, wide intercellular spaces in stratum basale, vacuolated cytoplasm and pyknotic nuclei in the stratum spinosum (Figure 7b). Massive granulation tissue was found in the wound bed with massive infiltration of inflammatory cells as well as many congested blood vessels with mild deposition of fine collagen fibers and increased number of spindle shaped cells (myofibroblasts) with absent skin appendages in wound area (Figure 8b). Group III showed wound surface covered by regenerated thin epidermis at the edge of wound area which is covered by scab (Figure 7c). At higher magnification, the epidermis showed more organized keratinocytes, vacuolated cytoplasm and few pyknotic nuclei in the stratum spinosum and few keratohyaline granules in stratum granulosum layer (Figure 7c). The wound bed is filled with moderate granulation tissue. Moderate infiltration of inflammatory cells and blood vessels were seen in the wound dermis with deposition of fine collagen fibers. It is also showed increased number of large spindle shaped fibroblasts and increased number of cells with large basophilic granules (mast cells) with absent skin appendages in the wound area (Figure 8c). Group IV showed regenerated epidermis on wound surface (Figures 7d, 8d). At higher magnification, the epidermis showed organized keratinocytes, some cells show vacuolated cytoplasm in the stratum spinosum and a few keratohyaline granules in stratum granulosum layer (Figure 7d). Mild inflammatory cell infiltrate as well as few newly formed blood vessels were found in the dermis. Papillary layer displayed prominent deposition of fine collagen fibers. Reticular layer has thick collagen bundles with emergence of regenerating hair follicles and high deposition of large spindle shaped fibroblast cells (Figure 8d).

On day 14, Group I showed regenerated thin epidermis with keratin at wound edge covering most of the wound surface (Figures 9a, 10a). At higher magnification, histological sections showed thin epidermis with disorganized keratinocytes, few cells showed vacuolated cytoplasm & few pyknotic nuclei in stratum spinosum layer were detected and minimal keratohyaline granules were seen in stratum granulosum layer with a small area of the wound surface lacking epidermis (Figure 9a). The wound bed contained massive granulation tissue. Massive infiltration of inflammatory cells and small blood vessels were identified in the dermis with absent skin appendages in the wound area (Figure 10a). Group II clarified regenerated thick epidermis with keratin at wound edge covering the wound surface (Figures 9b, 10b). At higher magnification, thick epidermis with organized keratinocytes was seen. Wide intercellular spaces in the stratum basale, vacuolated cytoplasm & pyknotic nuclei in stratum spinosum layer and few keratohyaline granules in stratum granulosum layer were recognized (Figure 9b). The wound bed is filled with moderate granulation tissue. Moderate infiltration of inflammatory cells and moderate blood vessels were observed in the dermis. Papillary layer showed prominent deposition of fine collagen strands. Reticular layer has thick interlacing collagen bundles. It also showed high deposition of large spindle shaped fibroblast cells and absence of skin appendages in the wound area (Figure 10b). Group III showed wound surface covered by regenerated well-formed epidermis which is covered by keratin at the edge of the wound with well-organized keratinocytes and moderate keratohyaline granules in stratum granulosum layer at high power magnification (Figure 9c). The wound bed contains minimal granulation tissue. Mild infiltration of inflammatory cells and moderate reformed blood vessels were identified in the dermis (Figures 9c, 10c). Papillary layer displayed fine interlacing collagen fibers. Reticular layer has thick collagen bundles with increased number of large spindle shaped fibroblasts and emergence of regenerating hair follicles (Figure 10c). Group IV showed thick complete regenerated epidermis which is covered by keratin covering the wound surface (Figures 9d, 10d). At higher magnification, thick regenerated epidermis with well organised keratinocytes and moderate keratohyaline granules in stratum granulosum layer were detected (Figure 9d). Very few infiltrations of inflammatory cells and moderate complete regenerated blood vessels were seen in the dermis. Papillary layer showed many delicate interlacing collagen fibers. Reticular layer has thick more organized collagen bundles running in different directions. Regenerated hair follicles were detected with increased number of large spindle shaped fibroblasts (Figures 9d, 10d).

On day 30, Group I showed wound surface covered with regenerated complete epidermis covered by keratin with few keratohyaline granules in the stratum granulosum and some cells showed vacuolated cytoplasm in stratum spinosum layer. Minimal infiltration of inflammatory cells with few newly formed blood vessels were identified in the dermis with absent skin appendages in the wound area. Abundant tiny, interlacing collagen fibers were visible in papillary layer. Reticular layer displayed thick collagen bundles (Figure 11a). Group II showed the same results as group I but with moderate reformed blood vessels were seen in the dermis and increased number of large spindle shaped fibroblasts (Figure 11b). Group III showed wound surface covered by regenerated well-formed complete epidermis which is covered by keratin with abundant keratohyaline granules in stratum granulosum layer. Moderate regenerated blood vessels were seen in the dermis. A lot of tiny, interlacing collagen fibers were visible in papillary layer. Reticular layer has thick organized collagen bundles running in different directions (Figures 11c,d). Increased number of large spindle shaped fibroblasts was detected (Figure 11c) with presence of complete regenerated hair follicles and sebaceous gland (Figures 11c,d). Group IV showed the same results as group III. Reticular layer displayed thick more organized collagen bundles running in different directions and complete regenerated well developed hair follicles and sebaceous gland (Figures 11e,f).

Masson's trichrome stain

Group A (negative control group) revealed extensive deposition of of dense thick well organized collagen bundles (blue colour) running in different directions like a meshwork in the dermis (Figure 12) with a statistically significant increase in its percentage (73.19 ± 6.17%), (73.86 ± 6.13%), (74.35 ± 6.73%) on days 7, 14 and 30 respectively (Figure 16).

On day 7, group I (positive control group) revealed scanty fine pale collagen fibers (blue colour) running in one direction in the dermis with percentage (13.24 ± 4.13%) (Figure 13a). Group II (PRP group) demonstrated few fine pale collagen fibers passing in one direction parallel to each other in the regenerated dermis (Figure 13b) with a statistically significant increase in its percentage (19.58 ± 2.99%) in relation to group I. Group III (Stem cells group) showed mild deposition of fine collagen fibers running in one direction in the regenerated dermis (Figure 13c) with a statistically significant increase in its percentage (34.06 ± 3.37%) relative to groups I, II. Group IV (PRP+ stem cells group) demonstrated moderate deposition of dense collagen bundles running in different directions in the regenerated dermis (Figure 13d) with a statistically significant increase in its percentage (42.38 ± 3.97%) in comparison with other diabetic study groups (B) (Figure 16). On day 14, group I showed mild deposition of fine collagen bundles running in one direction in the reformed dermis with percentage (27.51 ± 2.78%) (Figure 14a). Group II demonstrated more significant collagen bundle deposition running in one direction in the reformed dermis (Figure 14b) with a statistically significant increase in its percentage (43.10 ± 1.80%) relative to group I. Group III revealed moderate dense collagen bundles being deposited running in different directions in the reformed dermis (Figure 14c) with a statistically significant increase in

its percentage (54.90 ± 3.32%) in relation to groups I, II. Group IV displayed massive deposition of thick well organized collagen bundles running in different directions in the regenerated dermis (Figure 14d) with a statistically significant increase in its percentage (62.38 ± 0.94%) relative to other diabetic groups (Figure 16). On day 30, group I showed moderate deposition of thick bundles of collagen running in a single direction in the reformed dermis with percentage (44.43 ± 2.61%) (Figure 15a). Group II demonstrated more significant deposition of thicker collagen bundles running in a single direction in the reformed dermis (Figure 15b) with a statistically significant increase in its percentage (53.06 ± 2.62%) relative to group I. Group III revealed massive dense collagen bundle deposition running in different directions in the reformed dermis (Figure 15c) with a statistically significant increase in its percentage (61.48 ± 1.02%) relative to groups I, II. Group IV showed massive deposition of dense thick well organized collagen bundles running in many directions like a meshwork in the reformed dermis (Figure 15d) with a statistically significant increase in its percentage (69.31 ± 1.12%) compared to other diabetic groups (Figure 16). The percentage in group IV was closer to normal level (group A) as there was no significant statistical difference between both groups.

Immunohistochemical results

Immunohistochemical evaluation of CD68 macrophages in dermis of normal skin in rats of group A (negative control group) showed very few positive immunoreacted CD68 macrophages (brown dots) (Figure 17) with statistically significant decrease in its mean number (1.65 ± 0.27), (1.68 ± 0.26), (1.68 ± 0.26) on days 7, 14 and 30 respectively (Figure 21).

On day 7, immunohistochemical evaluation of CD68 macrophages in dermis of the induced skin wound demonstrated a numerous strong positive immunoreacted CD68 macrophages (brown dots) in group I (positive control group) (Figure 18a) and group II (PRP group) (Figure 18b). A statistically significant decline in CD68 macrophages count was seen in group II (40.40 ± 1.86) compared to group I (50.18 ± 1.69) ($p \leq 0.05$). Group III (stem cells group) demonstrated moderately positive immunoreacted cells (Figure 18c) with statistically significant decrease in its mean number (22.74 ± 1.97) in relation to groups I, II. Group IV (PRP+ stem cells group) revealed mildly positive immunoreacted cells (Figure 18d) with statistically significant decrease in its mean number (14.09 ± 1.41) relative to other diabetic studied groups (Figure 21). On day 14, immunohistochemical evaluation revealed a moderately positive immunoreacted CD68 macrophages in group I (Figure 19a) and group II (Figure 19b). A statistically significant decline in CD68 macrophages count was seen in group II (26.16 ± 0.85) compared to group I (30.90 ± 2.49) ($p \leq 0.05$). Group III demonstrated mildly positive immunoreacted cells (Figure 19c) with statistically significant decrease in its mean number (12.71 ± 1.03) relative to groups I, II. Group IV revealed few positive immunoreacted cells (Figure 19d) with statistically significant decrease in its mean number (9.22 ± 0.93) in relation to other diabetic studied groups (Figure 21). On day 30, immunohistochemical evaluation revealed a mildly strong positive immunoreacted CD68 macrophages in group I and group II (Figures 20 a,b respectively). A statistically significant decline in CD68 macrophages count was noted in group II (17.30 ± 1.29) compared to group I (22.06 ± 1.89) ($p \leq 0.05$). Groups III, IV demonstrated scanty immunoreacted cells (Figures 20 c,d respectively) with statistically significant decline in its mean number in group III (3.18± 0.83) relative to groups I&II. Statistically significant decline in the mean number in group IV (2.26 ± 0.64) was noted relative to groups I, II (Figure 21). The mean number in groups III, IV was close to normal level in group A.

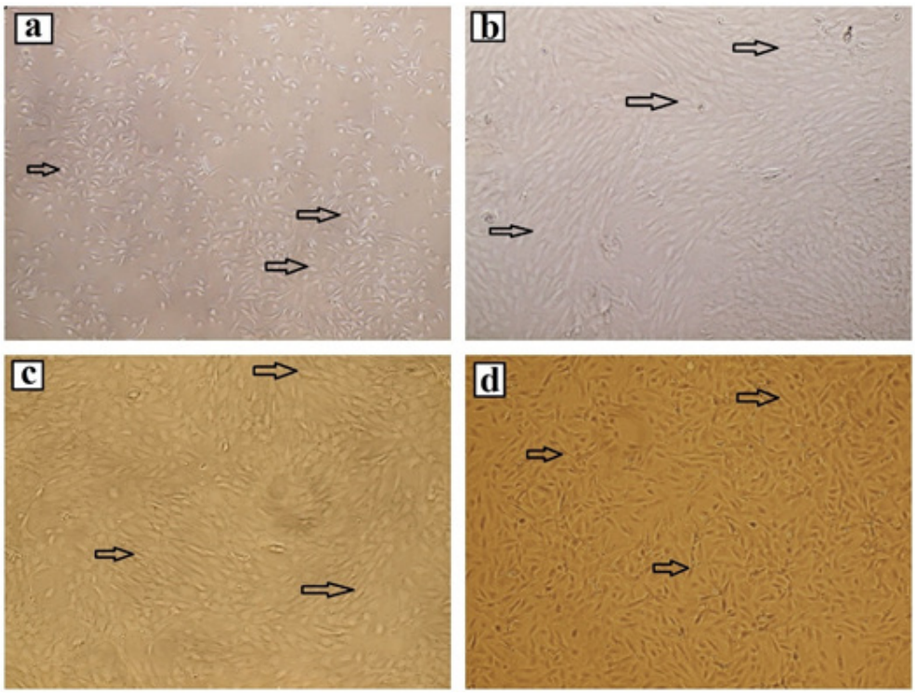

Fig. 1: Photomicrographs of BM-MSCs showing large, flattened spindle shaped fibroblast like cells. (a): Passage 0 that shows adherent fusiform cells with small cytoplasmic projections at 50% confluence. (b): Passage 1 that shows spindle shaped cells with 60% confluence. (c): Passage 2 that shows large spindle shaped cells at 70% confluence. (d): Passage 3 that shows large spindle shaped cells with 80% confluence. [Inverted phase contrast microscope, X100]

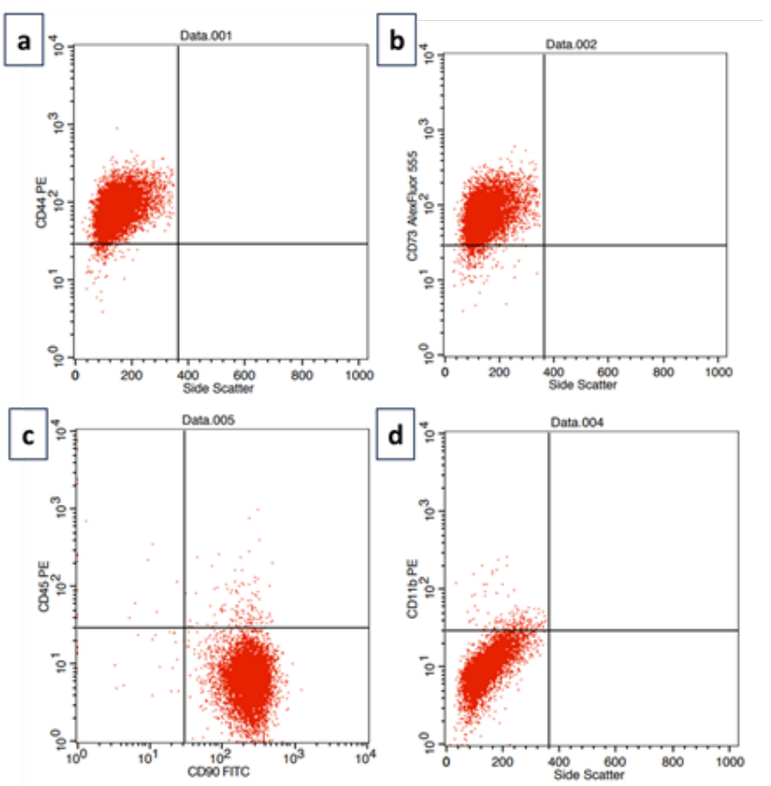

Fig. 2: A representative flow cytometry analysis of surface markers of cultured BM-MSCs at P3 showing: (a): High expression of CD44 (98.3%). (b): High expression of CD73 (96.6%). (c): High expression of CD90 (98%) and absence of expression of CD45 (2%). (d): Absence of expression of CD11/b (3%).

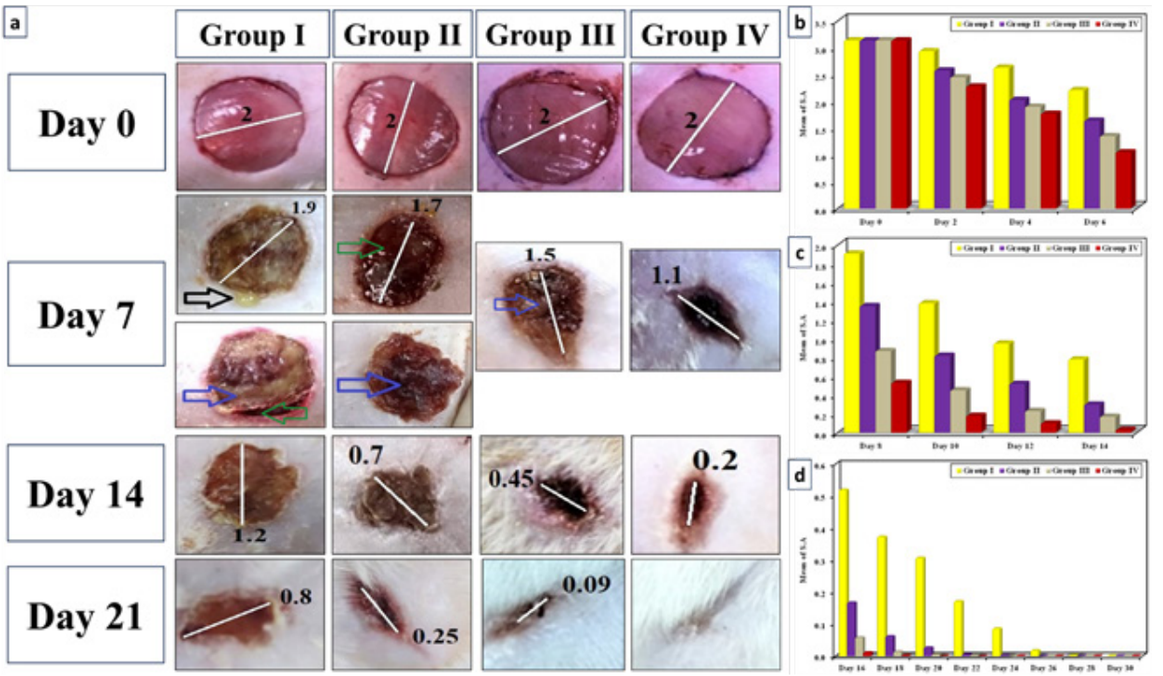

Fig. 3: (a): A photograph of induced skin wounds on the back of rats in group I (control), group II (PRP), group III (stem cells), and group IV (PRP + stem cells) taken at days 0, 7, 14, and 21. It shows anteroposterior diameters of induced skin wounds among the four groups measured in cm by FIJI/ImageJ software. The size of the wound area decreased obviously in all study groups compared to group I. Best and earliest healing was seen in group IV then group III then group II. Group I was the last to heal. Note pus exudate (black arrow) is seen in group I on day 7, redness in wound and its margins (green arrows) in groups I, II on day 7 and scab formation (blue arrows) in groups I, II, III on day 7. (b, c, d): Bar charts showing comparison between the study groups regarding mean of surface area of skin wound in the first week, in the second week and in last two weeks of the study period respectively.

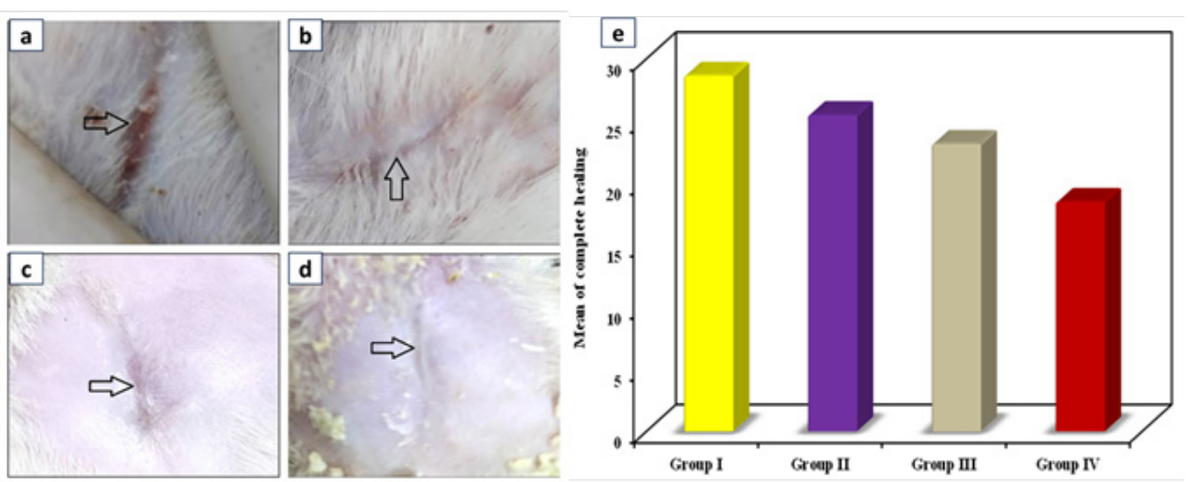

Fig. 4: Photograph of healed skin wounds (black arrows) on the back of rats in group I (a), group II (b), group III (c), and group IV (d) taken at day 30. (a): shows obvious red scar in group I, (b): shows less prominent scar in group II. (c, d): show well healed skin wounds with intact skin in groups III, IV. (e): A bar chart showing comparison between the study groups regarding time of complete healing of the skin wounds.

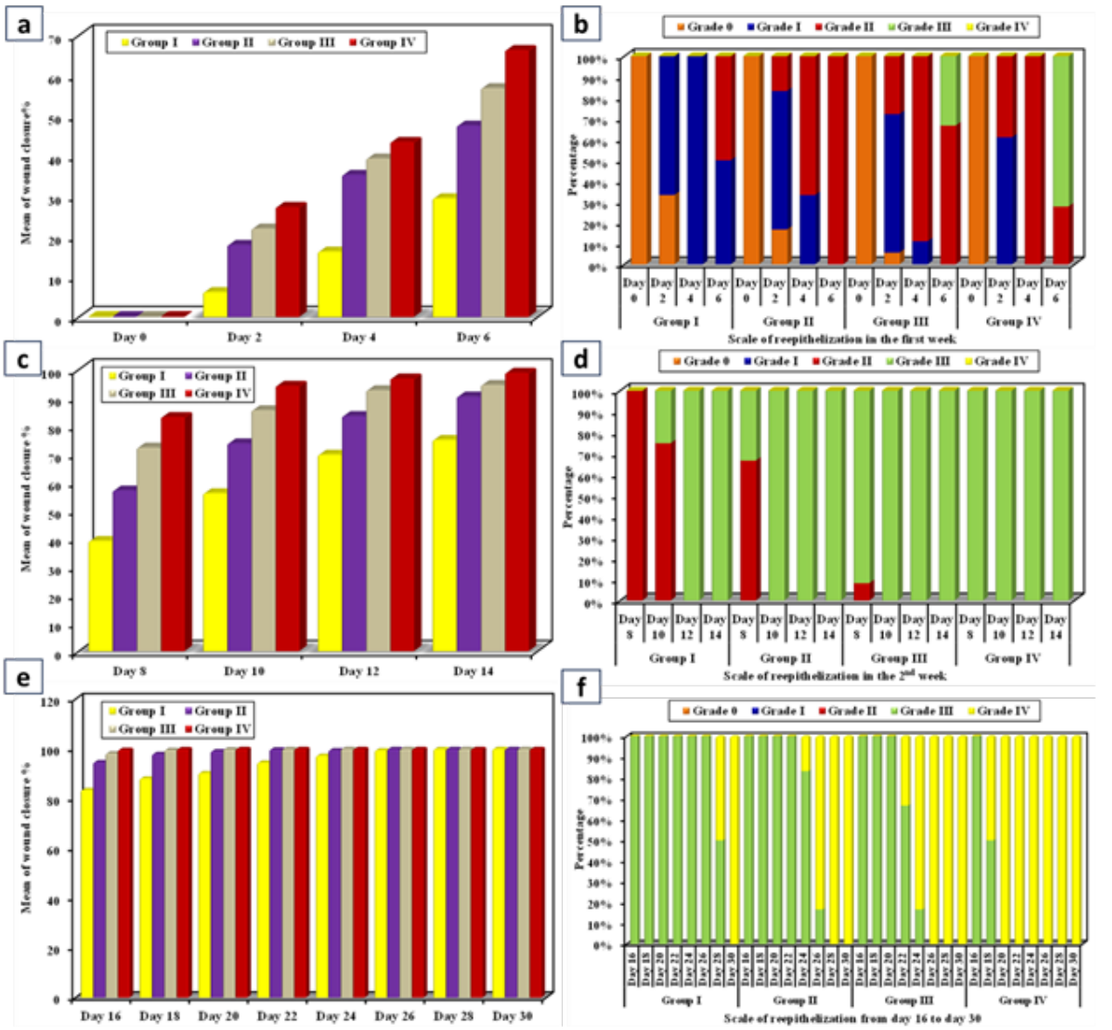

Fig. 5: (a, c, e): Bar charts showing comparison between the study groups regarding wound closure % in the first week, in the second week and in last two weeks of the study period respectively. (b, d, f): Bar charts showing comparison between the study groups regarding scale of reepithelization in the first week, in the second week and in last two weeks of the study period respectively.

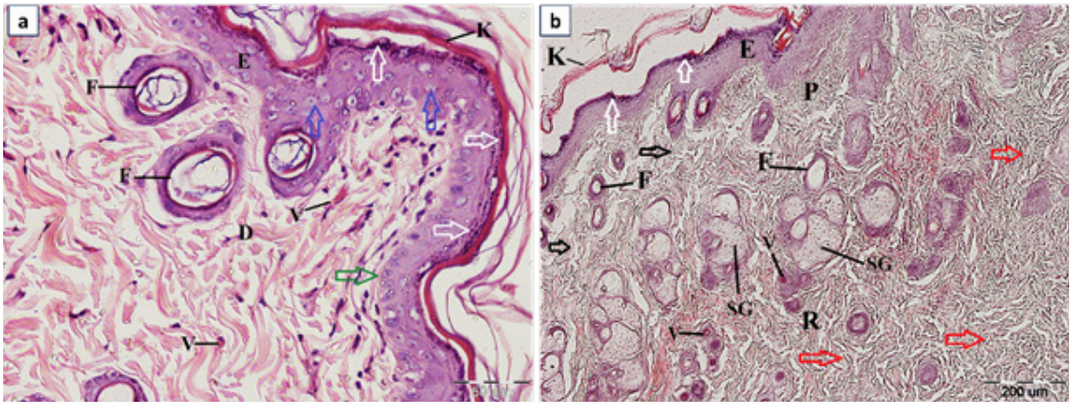

Fig. 6: Photomicrographs of normal histological structure of the skin in rats of group A (negative control group). (a): High magnification of epidermis showed thick epidermis (E) covered by keratin (K) with well-organized keratinocytes (blue arrows) lying on intact basement membrane (green arrow). Abundant keratohyaline granules (white arrows) were detected in stratum granulosum layer. Blood vessels (V) and a lot of hair follicles (F) were found in the underlying dermis (D). (b): Low magnification showed thick epidermis (E) covered by keratin (K) covering the dermis with a lot of keratohyaline granules (white arrows). Abundant hair follicles (F) and sebaceous glands (SG) were found in the dermis. Papillary layer (P) showed abundant deposition of fine interlacing collagen fibers (black arrows). The reticular layer (R) has thick organized collagen bundles (red arrows) running in different directions. [H&E stain, a X400, b X100]

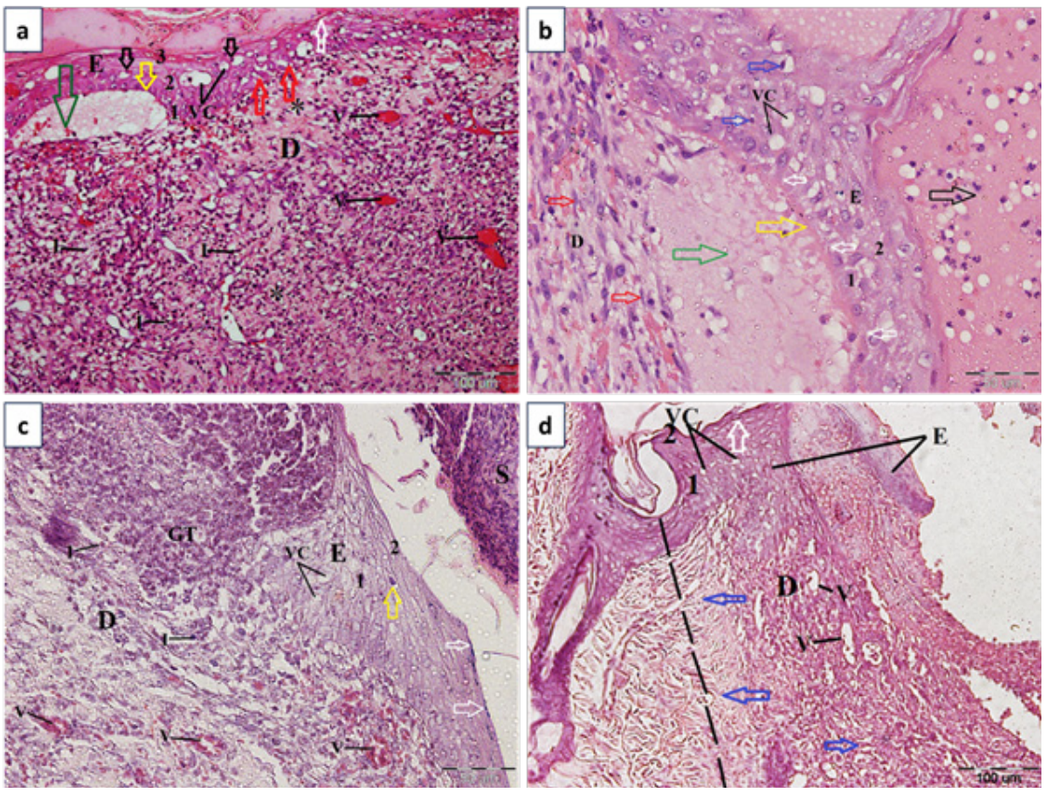

Fig. 7: Photomicrographs of the epidermis (E) of induced skin wounds in diabetic rats on day 7. (a): The epidermis of group I (positive control group) showed disorganized keratinocytes lying on an intact basement membrane (yellow arrow). Wide intercellular spaces (red arrows) in the stratum basale (1), vacuolated cytoplasm (VC) and pyknotic nuclei (black arrows) were detected in stratum spinosum layer (2) and the stratum granulosum layer (3) showed a few keratohyaline granules (white arrow). Areas of large fluid filled spaces (green arrow) seen between epidermis and underlying dermis (D) that showed massive inflammatory cell infiltration (I), congested blood vessels (V) and minimal fine collagen deposition (*). (b): The epidermis of group II (PRP group) showed disorganized keratinocytes lying on an intact basement membrane (yellow arrow), wide intercellular spaces (white arrows) in stratum basale (1), vacuolated cytoplasm (VC) and pyknotic nuclei (blue arrows) in the stratum spinosum (2). The epidermis is covered by exudation (black arrow). Areas of large fluid filled spaces (green arrows) were seen between epidermis and underlying dermis (D) that showed increased number of spindle shaped cells (myofibroblasts) (red arrows). (c): Group III (stem cells group) showed thin epidermis (E) at the edge of wound area which is covered by scab (S). It showed more organized keratinocytes, vacuolated cytoplasm (VC) and few pyknotic nuclei (yellow arrow) in the stratum spinosum (1) and few keratohyaline granules (white arrows) in stratum granulosum layer (2) covering moderate granulation tissue (GT). Moderate inflammatory cell infiltrate (I) and moderate blood vessels (V). (d): group IV (PRP + stem cells) showed thick epidermis (E). It showed organized keratinocytes, some cells show vacuolated cytoplasm (VC) in the stratum spinosum (1) and a few keratohyaline granules (white arrow) in stratum granulosum layer (2) covering mild infiltrate of inflammatory cells (I), few newly formed blood vessels (V) and thick collagen fibers (blue arrows) in underlying dermis (D). Dotted line: link between normal skin and twound area.

[H&E stain, a, b, c X400, d X200]

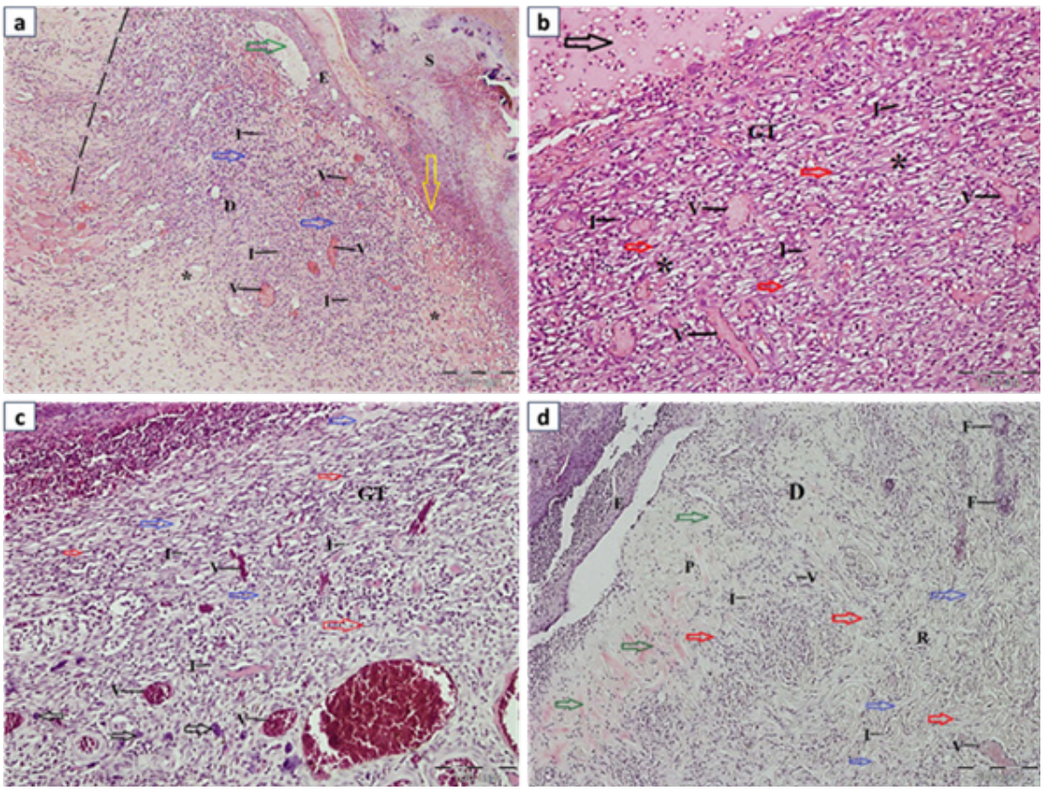

Fig. 8: Photomicrographs of the dermis of the induced skin wounds in diabetic rats on day 7.
(a): Group I (positive control group) showed most of the wound surface is covered by a scab (S) with absence of epidermis but intact basement membrane (yellow arrow) with thin epidermis (E) only at the edge of the wound. Areas of large fluid filled spaces (green arrow) seen between epidermis and underlying dermis (D). The wound bed filled with massive granulation tissue (blue arrows) with a massive inflammatory cell infiltration (I), congested blood vessels (V), and minimal fine collagen deposition (*). Note the absence of skin appendages. (b): Group II (PRP group) showed wound bed covered by exudation (black arrow) and filled with granulation tissue (GT), massive inflammatory cell infiltrate (I) and many congested blood vessels (V) with mild deposition of fine collagen fibers (*). Note the increased number of spindle shaped cells (myofibroblasts) (red arrows) and absent skin appendages. (c): Group III (stem cells group) showed the wound bed filled with moderate granulation tissue (GT). Moderate inflammatory cell infiltrate (I) and blood vessels (V) were found in the dermis. Note the deposition of fine collagen fibers (blue arrows). It also showed increased number of large spindle shaped fibroblasts (red arrows) and increased number of cells with large basophilic granules (mast cells) (black arrows). Note the absence of skin appendages in the wound area. (d): Group IV (PRP+ stem cells) showed regenerated epidermis (E) covering wound surface. Mild inflammatory cell infiltrate (I) and few newly formed blood vessels (V) were found in the dermis (D). Papillary (P) layer showed prominent deposition of fine collagen fibers (green arrows). The reticular (R) layer showed deposition of thick collagen bundles (blue arrows). Note the emergence of regenerating hair follicles (F) and deposition of large spindle shaped fibroblast cells (red arrows). Dotted line: link between normal skin and wound area.

[H&E stain, a, d X100, b, c X200]

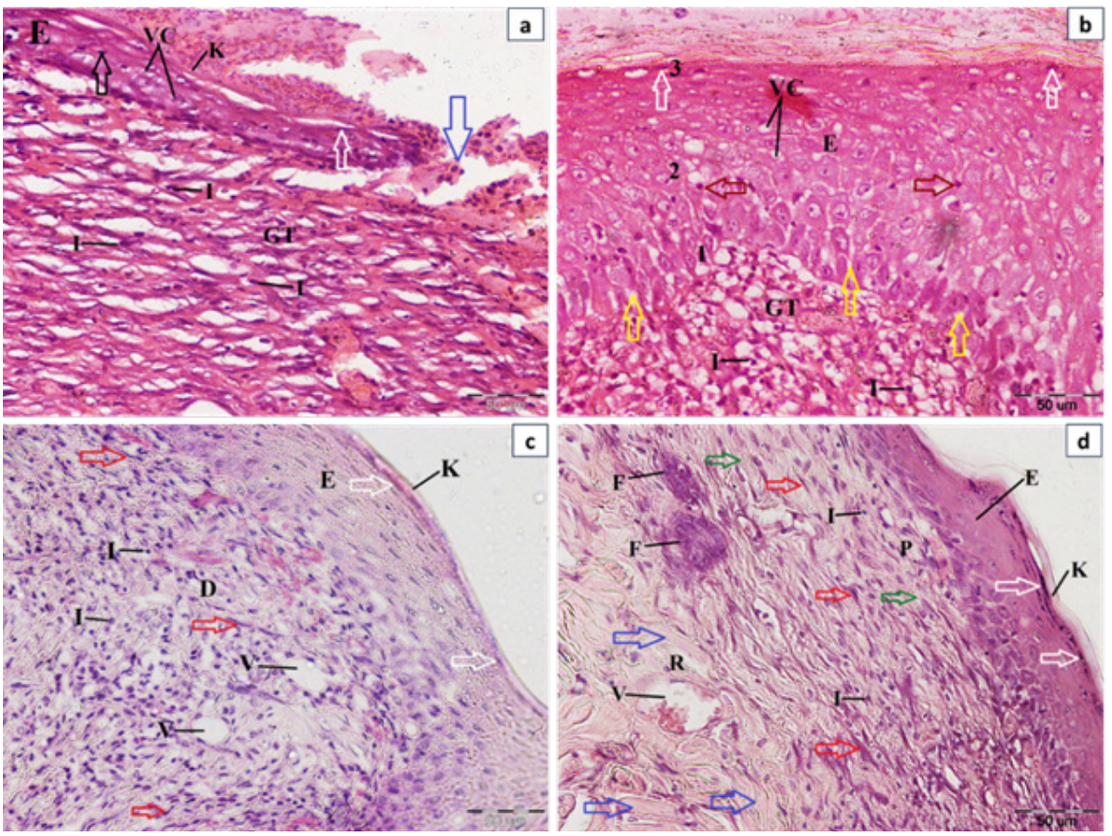

Fig. 9: Photomicrographs of the epidermis (E) of induced skin wounds in diabetic rats on day 14. (a): Group I (positive control group) showed regenerated thin epidermis (E) with keratin (K) at the edge of the wound covering most of the wound surface with disorganized keratinocytes. Few cells showed vacuolated cytoplasm (VC) & few pyknotic nuclei (black arrow) were detected in stratum spinosum layer and minimal keratohyaline granules were seen in stratum granulosum layer (white arrow) covering massive granulation tissue (GT) with massive inflammatory cell infiltrate (I). Note a small area of the wound surface not covered by epidermis (blue arrow). (b): Group II (PRP group) showed regenerated thick epidermis (E) with organized keratinocytes, keratin (K) at the edge of the wound, wide intercellular spaces (yellow arrows) in the stratum basale (1), vacuolated cytoplasm (VC) & pyknotic nuclei (red arrows) in stratum spinosum layer (2) and few keratohyaline granules (white arrows) in stratum granulosum layer (3) covering moderate granulation tissue (GT) and moderate inflammatory cell infiltrate (I). (c): Group III (stem cells group) showed regenerated well-formed epidermis (E) which is covered by keratin (K) at the edge of the wound with well-organized keratinocytes and moderate keratohyaline granules (white arrows) in stratum granulosum layer covering dermis (D) with mild inflammatory cell infiltrate (I) and moderate infiltration of newly formed blood vessels (V). Note the increased number of large spindle shaped fibroblasts (red arrows). (d): Group IV (PRP+ stem cells) showed thick complete regenerated epidermis (E) which is covered by keratin (K) with well organised keratinocytes and moderate keratohyaline granules in the stratum granulosum (white arrows) covering very few inflammatory cells infiltrate (I) and moderate complete regenerated blood vessels (V). Papillary (P) layer showed abundant fine interlacing collagen fibers (green arrows). The reticular (R) layer showed thick more organized collagen bundles (blue arrows) running in different directions. Note the presence of regenerated hair follicles (F) increased number of large spindle shaped fibroblasts (red arrows).

[H&E stain, a, b, c, d X400]

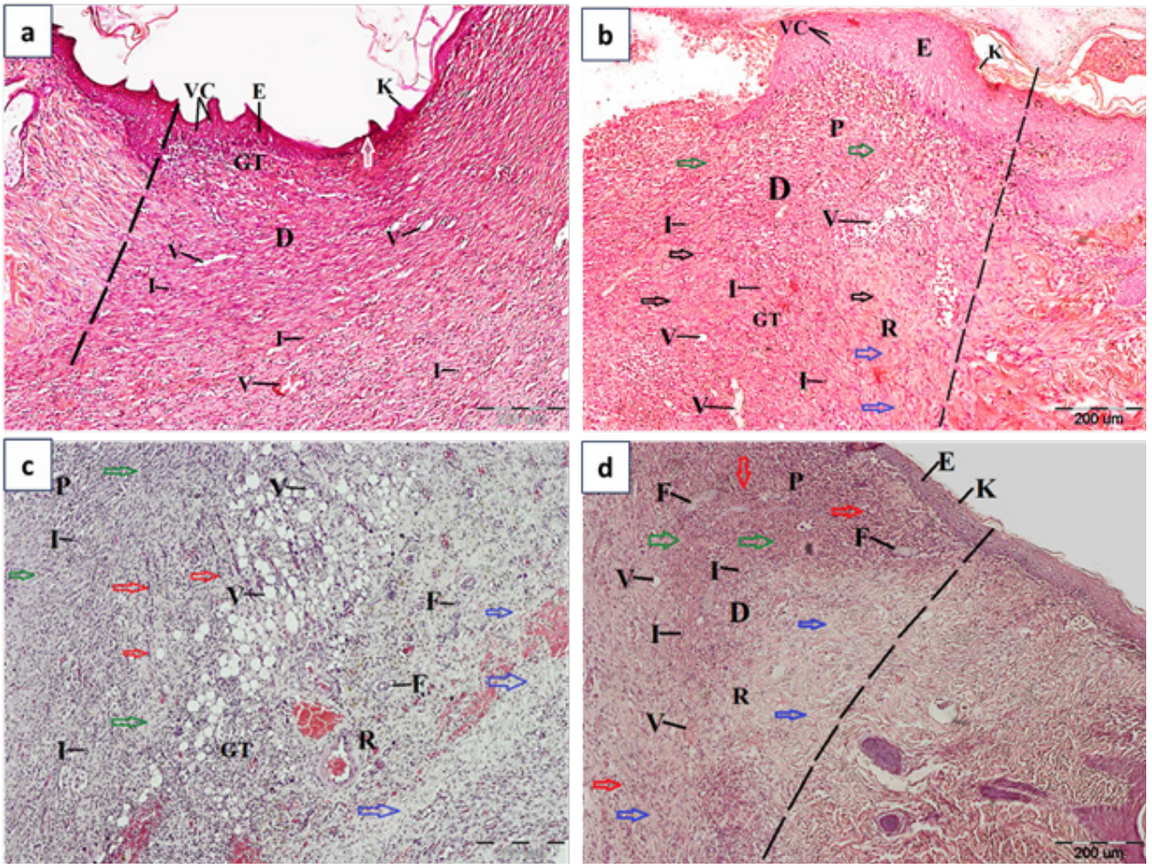

Fig. 10: Photomicrographs of the dermis of the induced skin wounds in diabetic rats on day 14
(a): Group I (positive control group) showed regenerated thin epidermis (E) with keratin (K) at the wound edge covering most of the wound surface with few cells showed vacuolated cytoplasm (VC) and minimal keratohyaline granules (white arrow). The wound bed is filled with massive granulation tissue (GT). Massive inflammatory cell infiltrate (I) and small blood vessels (V) were found in the dermis (D) with no skin appendages. (b): Group II (PRP group) showed regenerated thick epidermis (E) covering wound surface with keratin (K) at the edge of the wound and few cells showed vacuolated cytoplasm (VC). The wound bed is filled with moderate granulation tissue (GT). Moderate inflammatory cell infiltrate (I) and blood vessels (V) were found in the dermis (D). Papillary (P) layer showed prominent deposition of fine collagen fibers (green arrows). The reticular (R) layer showed interlacing collagen bundles (blue arrows). Note high deposition of large spindle shaped fibroblast cells (black arrows) and absent skin appendages. (c): Group III (stem cells group) showed the wound bed is filled with minimal granulation tissue (GT). Mild inflammatory cell infiltrate (I) and moderate infiltration of newly formed blood vessels (V) were found in the dermis (D). Papillary (P) layer showed fine interlacing collagen fibers (green arrows). The reticular (R) layer has thick collagen bundles (blue arrows). Note the increased number of large spindle shaped fibroblasts (red arrows) and presence of regenerated hair follicles (F). (d): Group IV (PRP+ stem cells) showed wound surface covered by thick complete regenerated epidermis (E) which is covered by keratin (K). Very few inflammatory cells infiltrate (I) and moderate complete regenerated blood vessels (V) were found in the dermis (D). Papillary (P) layer showed abundant fine interlacing collagen fibers (green arrows). The reticular (R) layer showed thick more organized collagen bundles (blue arrows) running in different directions. Note the presence of regenerated hair follicles (F) with increased number of large spindle shaped fibroblasts (red arrows).
Dotted line: link between normal skin and wound area.

[H&E stain, a, b, c, d X100]

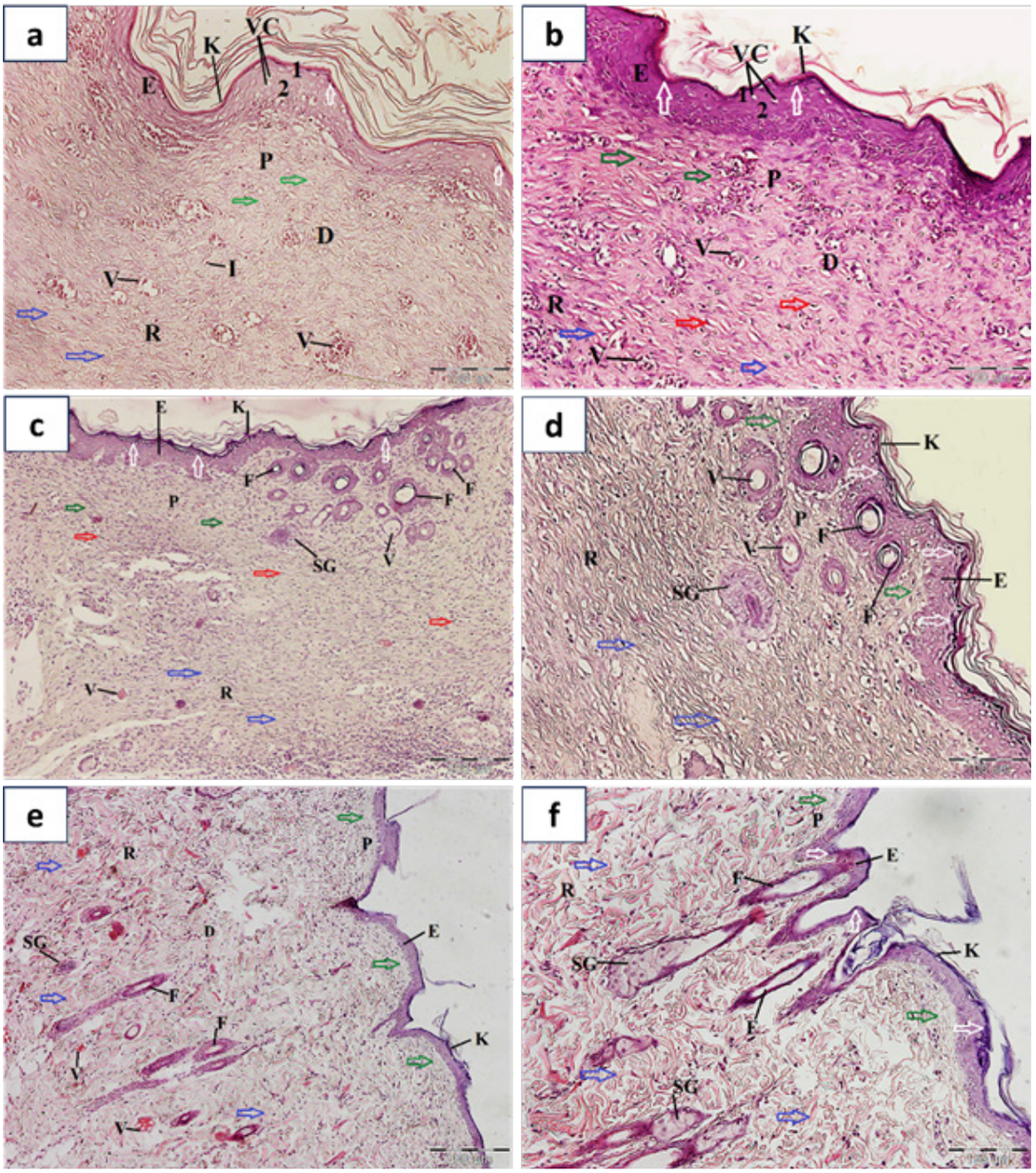

Fig. 11: Photomicrographs of skin wounds in rats on day 30:
(a): Group I (positive control group) showed regenerated complete epidermis (E) covered by keratin (K) covering wound surface with few keratohyaline granules (white arrows) in the stratum granulosum (1) and some cells show vacuolated cytoplasm (VC) in stratum spinosum layer (2). Minimal inflammatory cell infiltrate (I) and few newly formed blood vessels (V) were found in the dermis. The papillary layer (P) showed abundant deposition of fine interlacing collagen fibers (green arrows). The reticular layer (R) showed thick collagen bundles (blue arrows). (b): Group II (PRP) showed the same as (a) with moderate newly formed blood vessels (V) were seen in the dermis and increased number of large spindle shaped fibroblasts (red arrows). (c & d): Group III (stem cells) showed wound surface covered by regenerated well-formed complete epidermis (E) which is covered by keratin (K) with abundant keratohyaline granules (white arrows) in stratum granulosum layer. Moderate regenerated blood vessels (V) were found in the dermis. Papillary layer (P) showed abundant deposition of fine interlacing collagen fibers (green arrows). The reticular layer (R) has thick organized collagen bundles running in different directions (blue arrows). Note the increased number of large spindle shaped fibroblasts (red arrows) and presence of complete regenerated hair follicles (F) and sebaceous gland (SG). (e & f): Group IV (PRP+ stem cells) showed the same as (c & d). The reticular layer (R) has thick more organized collagen bundles (blue arrows) running in different directions and complete regenerated well developed hair follicles (F) and sebaceous gland (SG).

[H&E stain, a, b, d &f X200, c, e X100]

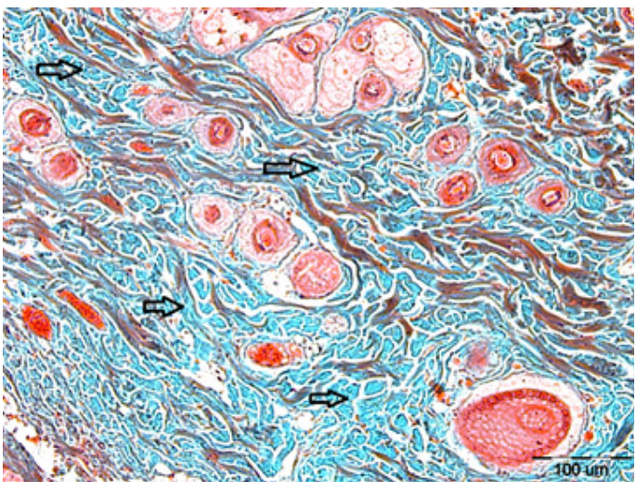

Fig. 12: Photomicrograph of normal skin in rats of group A (negative control group) showed extensive deposition of of dense thick well organized collagen bundles running in different directions like a meshwork in the dermis. Black arrows: collagen bundles (blue colour).

[Masson's trichrome stain, X200]

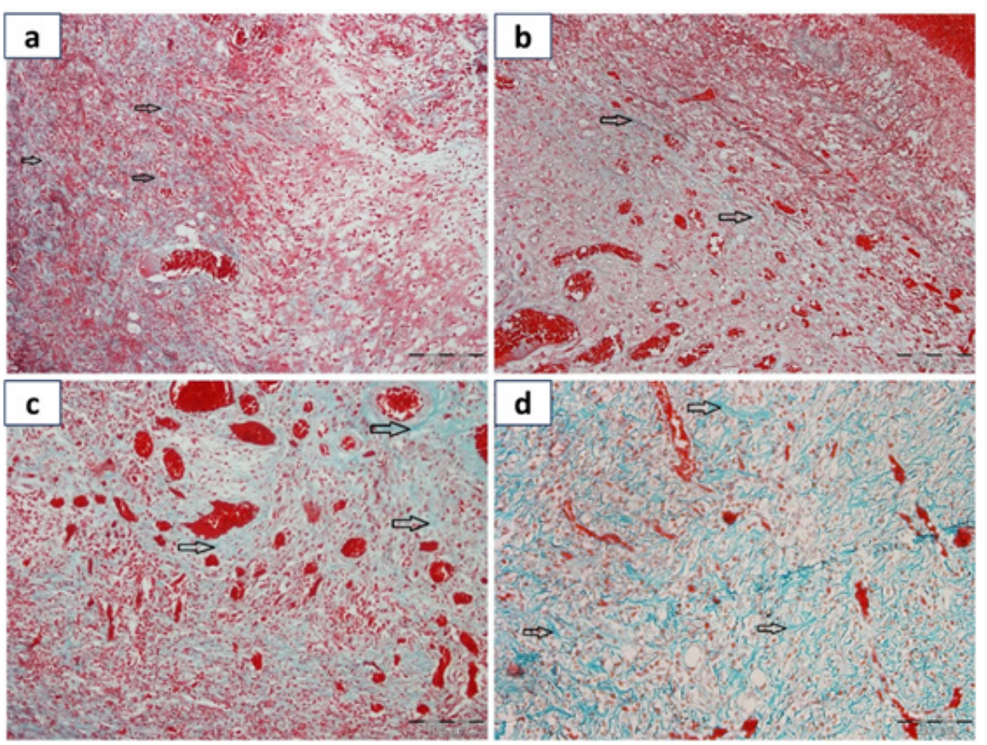

Fig. 13: Photomicrographs of the skin wound in the studied groups (B) on the 7th day. (a): Group I (positive control group) showed wound bed filled with scanty fine pale collagen fibers in the regenerated dermis passing in one direction. (b): Group II (PRP group) showed wound bed with few fine pale collagen fibers passing in one direction in the reformed dermis. (C): Group III (stem cells group) showed wound bed containing mild deposition of fine collagen fibers running in one direction in the reformed dermis. (d): Group IV (PRP+ stem cells group) showed the wound bed has moderate deposition of thick collagen bundles running in different directions in the regenerated dermis. Black arrows: collagen fibers and bundles (blue colour).

[Masson's trichrome stain, X200]

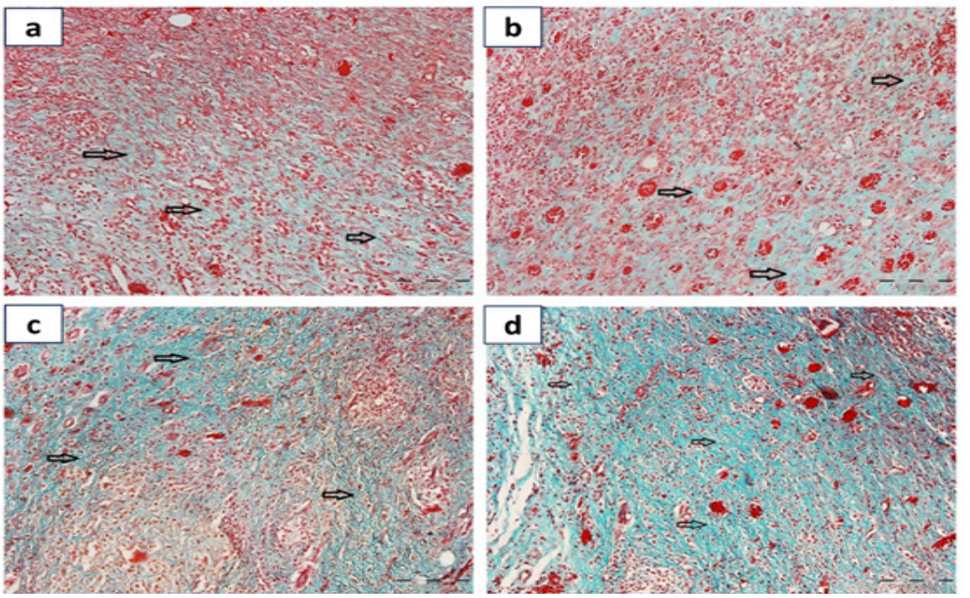

Fig. 14: Photomicrographs of the skin wound in the studied groups (B) on the 14th day. (a): Group I (positive control group) showed wound bed filled with mild deposition of fine collagen bundles running in one direction in the reformed dermis. (b): Group II (PRP group) showed prominent deposition of collagen bundles running in one direction in the reformed dermis. (c): Group III (stem cells) group showed moderate deposition of thick collagen bundles running in different directions in the regenerated dermis. (d): Group IV (PRP+ stem cells group) showed massive deposition of thick organized collagen bundles running in different directions in the regenerated dermis. Black arrows: collagen bundles (blue colour).

[Masson's trichrome stain, X200]

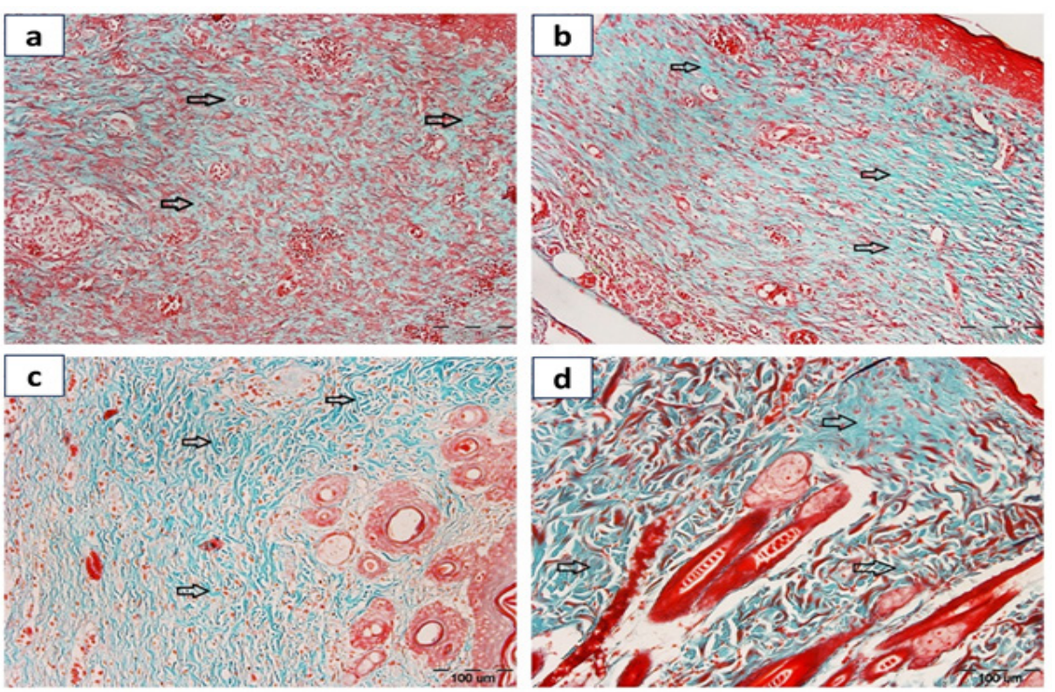

Fig. 15: Photomicrographs of the skin wound in the studied groups (B) on the 30th day. (a): Group I (positive control group) showed moderate deposition of thick collagen bundles running in one direction in dermis. (b): Group II (PRP group) showed more prominent deposition of thicker collagen bundles running in one direction in the reformed dermis. (c): Group III (stem cells group) showed massive deposition of thick collagen bundles running in different directions in the regenerated dermis. (d): Group IV (PRP+ stem cells group) showed massive deposition of dense thick well organized collagen bundles running in different directions like a meshwork in the regenerated dermis. Black arrows: collagen bundles (blue colour).

[Masson's trichrome stain, X200]

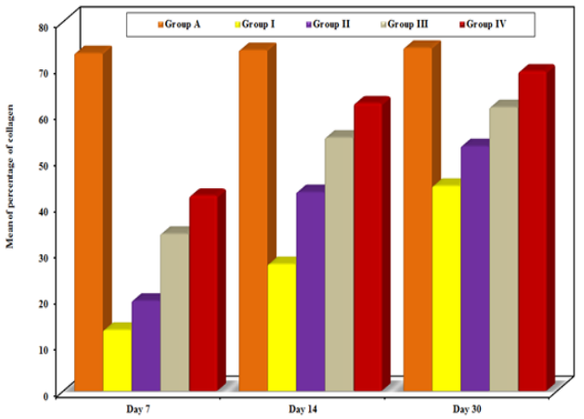

Fig. 16: A bar chart showing comparison between the study groups regarding percentage of collagen.

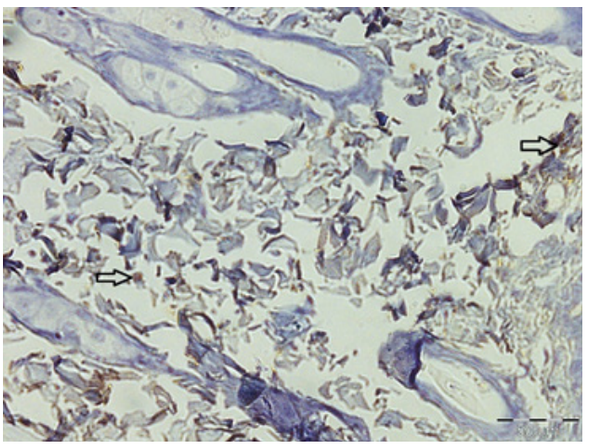

Fig. 17: Photomicrograph for immunohistochemical evaluation of CD68 macrophages (black arrows) in dermis of normal skin in rats of group A (negative control group) showed very few positive immunoreacted CD68 macrophages. [Anti CD68 counterstained with hematoxylin, X400]

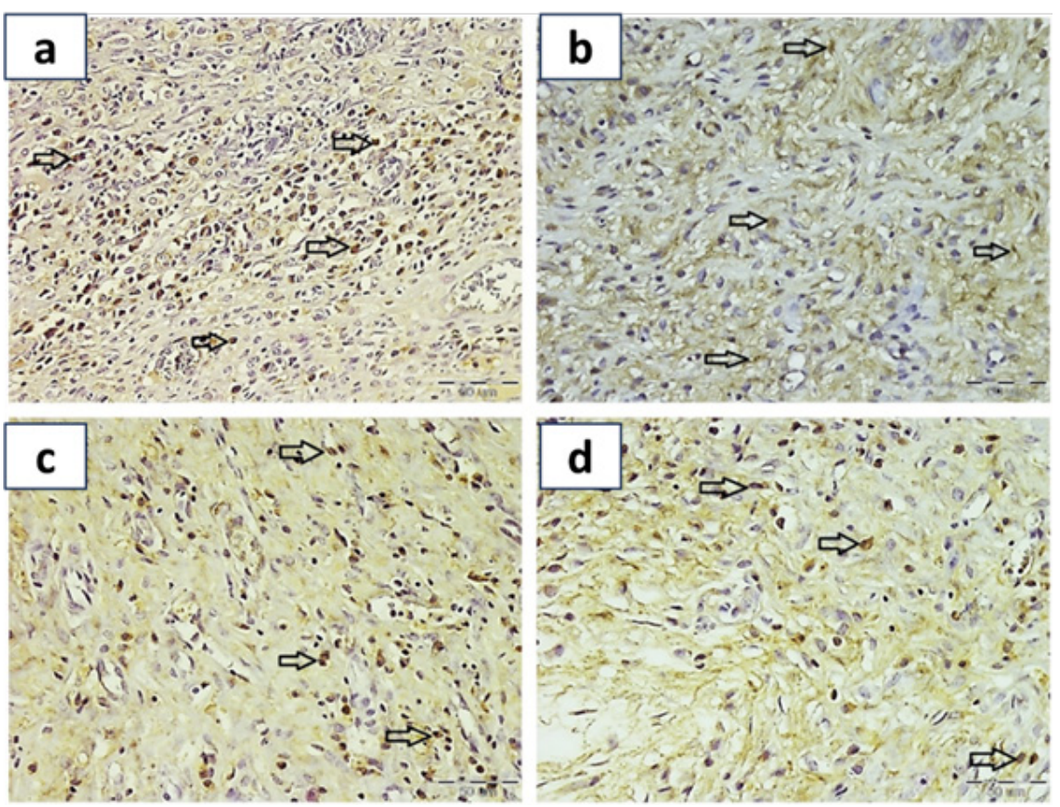

Fig. 18: Photomicrographs for immunohistochemical evaluation of CD68 macrophages (black arrows) in dermis of the induced skin wound on the 7th day in group I (a), group II (b), group III (c), and group IV(d). (a, b): show a numerous strong positive immunoreacted CD68 macrophages in groups I and II. (c): show moderately positive immunoreacted cells in group III. (d): show mildly positive immunoreacted cells in group IV.
[Anti CD68 counterstained with hematoxylin, X400]

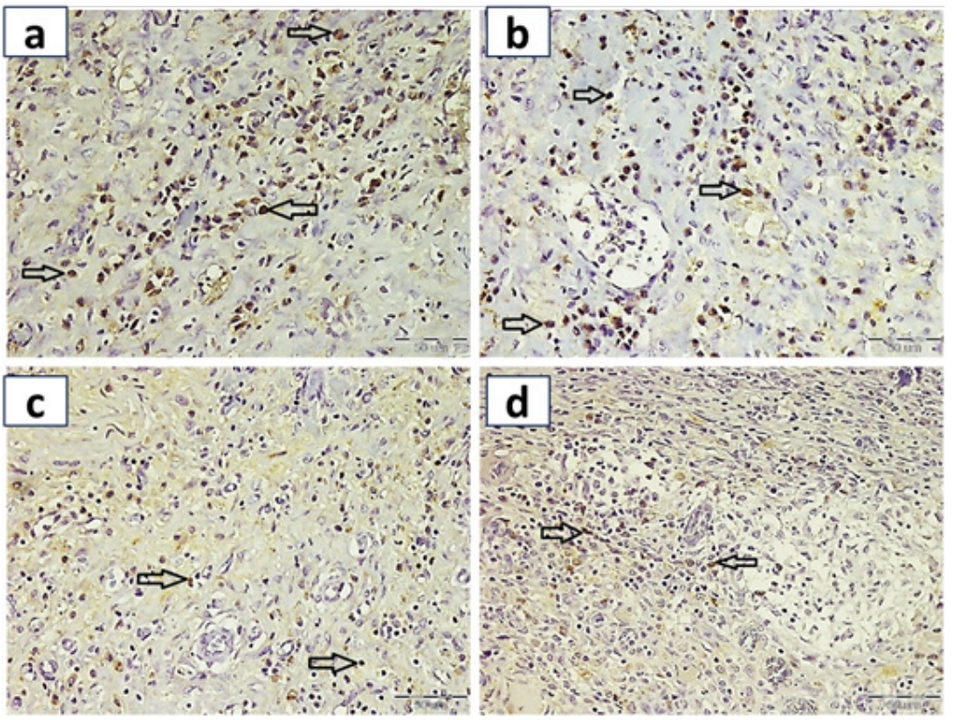

Fig. 19: Photomicrographs for immunohistochemical evaluation of CD68 macrophages (black arrows) in dermis of the induced skin wound on the 14th day in group I (a), group II (b), group III (c), and group IV (d). (a, b): show a moderately positive immunoreacted CD68 macrophages in groups I and II, (c): shows mildly positive immunoreacted cells in group III. (d): shows few positive immunoreacted cells in group IV.

[Anti CD68 counterstained with hematoxylin, X400]

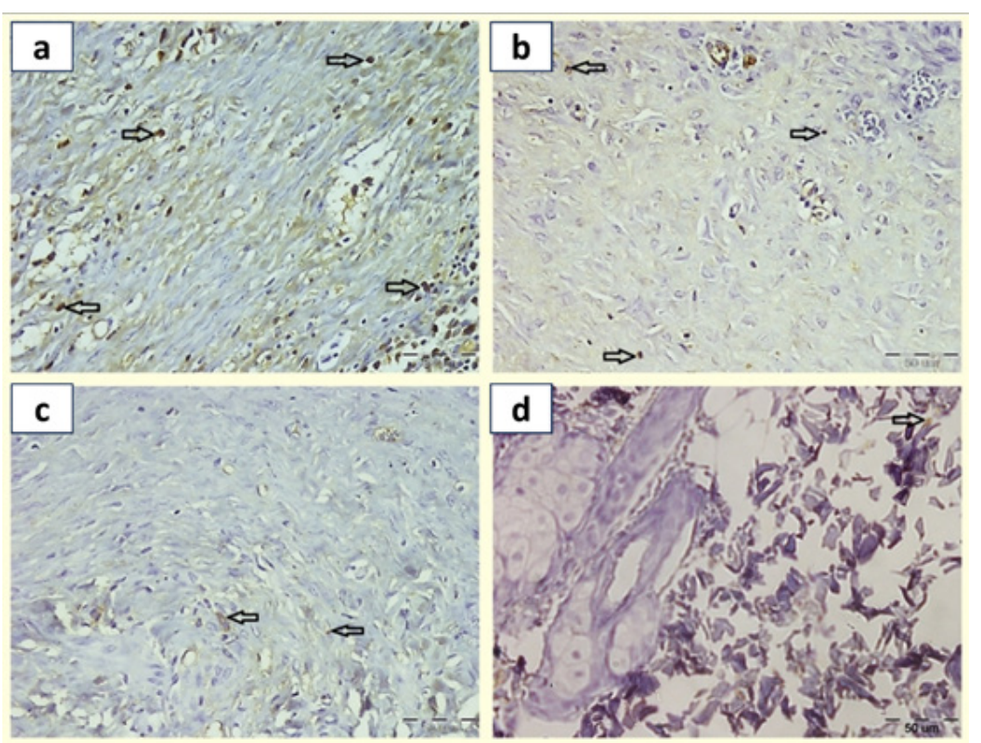

Fig. 20: Photomicrographs for immunohistochemical evaluation of CD68 macrophages (black arrows) in dermis of the induced skin wound on the 30th day in group I (a), group II (b), group III (c), and group IV (d). (a, b): show mildly positive immunoreacted CD68 macrophages in groups I and II. (c, d): show scanty immunoreacted cells in groups III and IV.

[Anti CD68 counterstained with hematoxylin, X400]

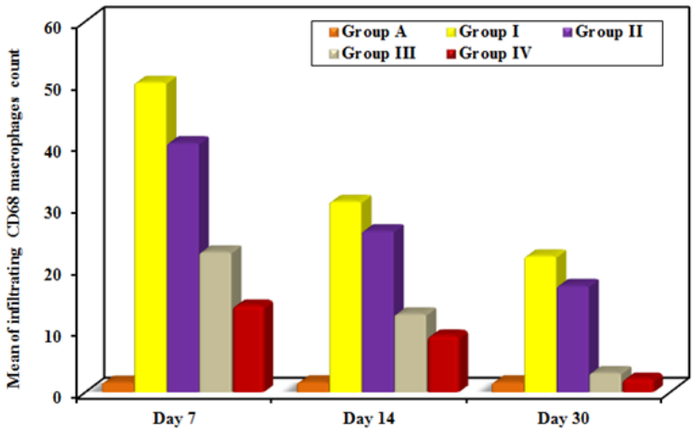

Fig. 21: A bar chart showing comparison between the study groups regarding Infiltrating CD68 macrophages count

Table 1: Comparison between the study groups regarding scale of reepithelization in the first week

Scale of reepithelization in the first week	Group I (n = 18)	Group II (n = 18)	Group III (n = 18)	Group IV (n = 18)	c^2	*p*
Day 0						
Grade 0	18 (100%)	18 (100%)	18 (100%)	18 (100%)		
Grade I	0 (0%)	0 (0%)	0 (0%)	0 (0%)		
Grade II	0 (0%)	0 (0%)	0 (0%)	0 (0%)	-	-
Grade III	0 (0%)	0 (0%)	0 (0%)	0 (0%)		
Grade IV	0 (0%)	0 (0%)	0 (0%)	0 (0%)		
Day 2						
Grade 0	6 (33.3%)	3 (16.7%)	1 (5.6%)	0 (0%)		
Grade I	12 (66.7%)	12 (66.7%)	12 (66.7%)	11 (61.1%)		
Grade II	0 (0%)	3 (16.7%)	5 (27.8%)	7 (38.9%)	15.370*	^{MC}p= 0.009*
Grade III	0 (0%)	0 (0%)	0 (0%)	0 (0%)		
Grade IV	0 (0%)	0 (0%)	0 (0%)	0 (0%)		
p_0		0.190	0.017*	0.001*		
Sig.bet.Grps			p_1=0.537, p_2=0.111, p_3=0.728			
Day 4						
Grade 0	0 (0%)	0 (0%)	0 (0%)	0 (0%)		
Grade I	18 (100%)	6 (33.3%)	2 (11.1%)	0 (0%)		
Grade II	0 (0%)	12 (66.7%)	16 (88.9%)	18 (100%)	46.957*	<0.001*
Grade III	0 (0%)	0 (0%)	0 (0%)	0 (0%)		
Grade IV	0 (0%)	0 (0%)	0 (0%)	0 (0%)		
p_0		<0.001*	<0.001*	<0.001*		
Sig.bet.Grps			p_1=0.228, p_2=0.019*, p_3=0.486			
Day 6						
Grade 0	0 (0%)	0 (0%)	0 (0%)	0 (0%)		
Grade I	9 (50%)	0 (0%)	0 (0%)	0 (0%)		
Grade II	9 (50%)	18 (100%)	12 (66.7%)	5 (27.8%)	49.801*	^{MC}p <0.009*
Grade III	0 (0%)	0 (0%)	6 (33.3%)	13 (72.2%)		
Grade IV	0 (0%)	0 (0%)	0 (0%)	0 (0%)		
p_0		0.001*	<0.001*	<0.001*		
Sig.bet.Grps			p_1=0.019*, p_2<0.001*, p_3=0.019*			

χ^2: Chi square test , MC: Monte Carlo *p*: *p value* for comparing between the studied groups

p_0: *p value* for comparing between Group I and each other group p_1: *p value* for comparing between Group II and III

p_2: *p value* for comparing between Group II and IV p_3: *p value* for comparing between Group III and IV *: Statistically significant at $p \leq 0.05$

Table 2: Comparison between the studied groups regarding scale of reepithelization in the 2nd week

Scale of reepithelization in the 2nd week	Group I (n = 12)	Group II (n = 12)	Group III (n = 12)	Group IV (n = 12)	c^2	*p*
Day 8						
Grade 0	0 (0%)	0 (0%)	0 (0%)	0 (0%)		
Grade I	0 (0%)	0 (0%)	0 (0%)	0 (0%)		
Grade II	12 (100%)	8 (66.7%)	1 (8.3%)	0 (0%)	33.439*	<0.001*
Grade III	0 (0%)	4 (33.3%)	11 (91.7%)	12 (100%)		
Grade IV	0 (0%)	0 (0%)	0 (0%)	0 (0%)		
p_0		0.093	<0.001*	<0.001*		
Sig.bet.Grps			p_1=0.009*, p_2=0.001*, p_3=1.000			
Day 10						
Grade 0	0 (0%)	0 (0%)	0 (0%)	0 (0%)		
Grade I	0 (0%)	0 (0%)	0 (0%)	0 (0%)		
Grade II	9 (75%)	0 (0%)	0 (0%)	0 (0%)	25.756*	^{MC}p <0.001*
Grade III	3 (25%)	12 (100%)	12 (100%)	12 (100%)		
Grade IV	0 (0%)	0 (0%)	0 (0%)	0 (0%)		
p_0		<0.001*	<0.001*	<0.001*		
Day 12						
Grade 0	0 (0%)	0 (0%)	0 (0%)	0 (0%)		
Grade I	0 (0%)	0 (0%)	0 (0%)	0 (0%)		
Grade II	0 (0%)	0 (0%)	0 (0%)	0 (0%)	-	-
Grade III	12 (100%)	12 (100%)	12 (100%)	12 (100%)		
Grade IV	0 (0%)	0 (0%)	0 (0%)	0 (0%)		
Day 14						
Grade 0	0 (0%)	0 (0%)	0 (0%)	0 (0%)		
Grade I	0 (0%)	0 (0%)	0 (0%)	0 (0%)		
Grade II	0 (0%)	0 (0%)	0 (0%)	0 (0%)	-	-
Grade III	12 (100%)	12 (100%)	12 (100%)	12 (100%)		
Grade IV	0 (0%)	0 (0%)	0 (0%)	0 (0%)		

χ^2: Chi square test , MC: Monte Carlo
p: *p value* for comparing between the studied groups
p_0: *p value* for comparing between Group I and each other group
p_1: *p value* for comparing between Group II and III
p_2: *p value* for comparing between Group II and IV
p_3: *p value* for comparing between Group III and IV
*: Statistically significant at $p \leq 0.05$

Table 3: Comparison between the studied groups regarding scale of reepithelization in last 2 weeks.

Scale of reepithelization from day 16 to day 30	Group I (n = 6)	Group II (n = 6)	Group III (n = 6)	Group IV (n = 6)	c^2	*p*
Day 16						
Grade 0	0 (0%)	0 (0%)	0 (0%)	0 (0%)		
Grade I	0 (0%)	0 (0%)	0 (0%)	0 (0%)		
Grade II	0 (0%)	0 (0%)	0 (0%)	0 (0%)	-	-
Grade III	6 (100%)	6 (100%)	6 (100%)	6 (100%)		
Grade IV	0 (0%)	0 (0%)	0 (0%)	0 (0%)		
Day 18						
Grade 0	0 (0%)	0 (0%)	0 (0%)	0 (0%)		
Grade I	0 (0%)	0 (0%)	0 (0%)	0 (0%)		
Grade II	0 (0%)	0 (0%)	0 (0%)	0 (0%)	6.371*	^{MC}p=0.039*
Grade III	6 (100%)	6 (100%)	6 (100%)	3 (50%)		
Grade IV	0 (0%)	0 (0%)	0 (0%)	3 (50%)		

Continue Table 3

p_0		-	-	0.182		
Sig.bet.Grps			p_1=-, p_2=0.182, p_3=0.182			
Day 20						
Grade 0	0 (0%)	0 (0%)	0 (0%)	0 (0%)		
Grade I	0 (0%)	0 (0%)	0 (0%)	0 (0%)		
Grade II	0 (0%)	0 (0%)	0 (0%)	0 (0%)	19.139*	^{MC}p<0.001*
Grade III	6 (100%)	6 (100%)	6 (100%)	0 (0%)		
Grade IV	0 (0%)	0 (0%)	0 (0%)	6 (100%)		
p_0		-	-	0.002*		
Sig.bet.Grps			p_1=-, p_2=0.002*, p_3=0.002*			
Day 22						
Grade 0	0 (0%)	0 (0%)	0 (0%)	0 (0%)		
Grade I	0 (0%)	0 (0%)	0 (0%)	0 (0%)		
Grade II	0 (0%)	0 (0%)	0 (0%)	0 (0%)	16.610*	<0.001*
Grade III	6 (100%)	6 (100%)	4 (66.7%)	0 (0.0%)		
Grade IV	0 (0.0%)	0 (0.0%)	2 (33.3%)	6 (100.0%)		
p_0		-	0.455	0.002*		
Sig.bet.Grps			p_1=0.455, p_2=0.002*, p_3=0.061			
Day 24						
Grade 0	0 (0.0%)	0 (0.0%)	0 (0.0%)	0 (0.0%)		
Grade I	0 (0.0%)	0 (0.0%)	0 (0.0%)	0 (0.0%)		
Grade II	0 (0.0%)	0 (0.0%)	0 (0.0%)	0 (0.0%)	17.110*	<0.001*
Grade III	6 (100%)	5 (83.3%)	1 (16.7%)	0 (0.0%)		
Grade IV	0 (0.0%)	1 (16.7%)	5 (83.3%)	6 (100.0%)		
p_0		1.000	0.015*	0.002*		
Sig.bet.Grps			p_1=0.080, p_2=0.015*, p_3=1.000			
Day 26						
Grade 0	0 (0.0%)	0 (0.0%)	0 (0.0%)	0 (0.0%)		
Grade I	0 (0.0%)	0 (0.0%)	0 (0.0%)	0 (0.0%)		
Grade II	0 (0.0%)	0 (0.0%)	0 (0.0%)	0 (0.0%)	17.154*	^{MC}p<0.001*
Grade III	6 (100%)	1 (16.7%)	0 (0.0%)	0 (0.0%)		
Grade IV	0 (0.0%)	5 (83.3%)	6 (100%)	6 (100%)		
p_0		0.015*	0.002*	0.002*		
Sig.bet.Grps			p_1=1.000, p_2=1.000, p_3=-			
Day 28						
Grade 0	0 (0.0%)	0 (0.0%)	0 (0.0%)	0 (0.0%)		
Grade I	0 (0.0%)	0 (0.0%)	0 (0.0%)	0 (0.0%)		
Grade II	0 (0.0%)	0 (0.0%)	0 (0.0%)	0 (0.0%)	6.371*	^{MC}p=0.042*
Grade III	3 (50%)	0 (0%)	0 (0%)	0 (0%)		
Grade IV	3 (50%)	6 (100%)	6 (100%)	6 (100%)		
p_0		0.182	0.182	0.182		
Sig.bet.Grps			p_1=-, p_2=-, p_3=-			
Day 30						
Grade 0	0 (0%)	0 (0%)	0 (0%)	0 (0%)		
Grade I	0 (0%)	0 (0%)	0 (0%)	0 (0%)		
Grade II	0 (0%)	0 (0%)	0 (0%)	0 (0%)	-	-
Grade III	0 (0%)	0 (0%)	0 (0%)	0 (0%)		
Grade IV	6 (100%)	6 (100%)	6 (100%)	6 (100%)		

χ^2: Chi square test , MC: Monte Carlo
p_0: *p value* for comparing between Group I and each other group
p_2: *p value* for comparing between Group II and IV
*: Statistically significant at $p \leq 0.05$
p: *p value* for comparing between the studied groups
p_1: *p value* for comparing between Group II and III
p_3: *p value* for comparing between Group III and IV

DISCUSSION

Despite major healthcare resources being dedicated to wound care, nonhealing wounds are linked to catastrophic side effects including scarring, disfigurement, life-threatening functional impairment and amputation in various wounds especially those of diabetic patients[8]. one to two percent of the world's population is affected by diabetic wounds, which cost 2.5 to 15 percent of annual global health budgets[33]. Diabetes mellitus causes insulin resistance, ongoing inflammation, and decreased cell proliferation in wounds[34]. The methods utilized to treat diabetic wounds at the moment emphasize reducing excessive inflammation and encouraging the proliferation of cells[35]. However, haemocytes, parenchymal cells proteins of extracellular matrix, and soluble mediators were all implicated in the wound healing process[36]. As a result, adopting a single approach to provide excellent outcomes is never easy. Therefore, the necessity for a perfect synergistic approach to solve the issue is crucial.

The present work was conducted to investigate and compare the potential therapeutic effect of locally injected bone marrow- derived mesenchymal stem cells (BM-MSCs) as well as platelet rich plasma (PRP) individually or combined in the healing of skin wound in induced diabetic albino rats.

Platelet-rich plasma is a compound which is derived from blood, and it possesses highly concentrated platelets in plasma. Centrifugation is used to separate it from blood. Activated platelets from PRP can secrete a lot of cytokines and many growth factors, including transforming growth factor-β (TGF-β), basic fibroblast growth factor (bFGF), platelet-derived growth factor (PDGF), insulin-like growth factor-1 (IGF-1), and vascular endothelial growth factor (VEGF) that aid in stimulating tissue regeneration and repair. PRP is used in many surgeries and clinical treatments as it is an easily accessible simply prepared cell therapy containing many bioactive growth factors with low immunogenicity, its therapeutic application can be achieved by simple techniques and its separation from whole blood is not expensive[11,37]. As a result, PRP was injected intralesional in the present work to indicate PRP effects on experimental cutaneous wounds in rats.

Because MSCs are readily extracted at clinical criteria from a variety of tissues, such as bone marrow and adipose tissues, and because they secrete a variety of soluble factors that has trophic, cytoprotective and anti-inflammatory properties, the use of MSCs is a powerful strategy for the repair of damaged tissues and organs. Additionally, the use of MSCs has been demonstrated to be secure and practical in the clinic[8,38].

In this study BM-MSCs were injected intralesional as it has also been widely applied in the treatment of wounds. As mentioned by Leonardi *et al*[39]. in their study, BM-MSCs in synthetic dermal substitutes improved wound healing. These stem cells were found to accelerate the process of reepithelialization and improve vascular density in the wounds as mentioned by Hu *et al*[40].

Albino Wistar strain rats were chosen as experimental animals in this study as they are larger in size compared to mice that leads to easy handling, sampling, and easy performed procedures as well as their similarity to humans regarding anatomical, physiological, and genetic features, also, they can resist infections[41]. Male rats were favoured to decrease the rapid impact of natural estrogens on the healing of wounds[42].

Streptozotocin (STZ) was chosen for induction of diabetes in the present work as it is currently most frequently used for diabetes induction in mice and rats due to its diabetogenic effects as it causes damage of pancreatic islet β-cells which results in insulin insufficiency, hyperglycemia, polydipsia, and polyuria which are indicative of diabetes mellitus as mentioned by Furman[43] in his study.

The dose of induction of diabetes in the present study was 40 mg/kg as it was the least and safest dose to induce diabetes with least mortality incidence based on the study of Kaur *et al*[28].

Full thickness surgical incision was done on the dorsum of rats to remove the endogenous stem cells effect that are located in hair follicles and sebaceous glands[44]. It involves lower immune responses and regeneration processes than other wound types, the sterile dermal incision is frequently regarded as the "simplest" wound type in the broad subject of tissue repair. In addition, the wounds were covered by tegaderm dressing as it prevents the harmful bacteria from invasion into the wound and reduces the inflammation response[6].

Haemostasis / inflammation, angiogenesis / cell proliferation, and remodelling are the three overlapping phases of the wound healing process as mentioned by Yan *et al*.[7] As a result, skin wound specimens were taken on day 7 to examine wound healing inflammatory phase, day 14 to assess the proliferative phase which matched with what was said by Ebrahim *et al*.[30] and on day 30 which was the end of research period to assess full recovery of wounds.

In the present work regarding the gross morphological results, it was demonstrated that the size of raw wound area (total surface area) statistically significant decreased as well as increase in percentage of wound closure and degree of reepithelization of statistical significance in groups (II, III, IV) relative to control group (group I) throughout the study period. Best healing results were seen in group III (stem cells) and group IV (combined stem cells and PRP) while PRP group (group II) showed a lesser grade of healing, but it was better than that of control group. Regarding mean time of complete healing, there was a difference of statistical significance between the four studied groups and between control group and the other study groups as group IV was the first group to reach complete healing in time ranged from day 17 to day 20 of the study period, followed by group III, then group II followed by group I that reached complete healing in range of time from day 28 to day 30 of the research period.

Cardinal signs of inflammation as redness of skin surrounding the wound edges obviously demonstrated in group I and with lesser extent in group II in this work. While groups III, IV showed the least inflammatory signs.

In the present study, signs of infection appeared only in group I (control group) at days 4 and 7 post surgery that manifested by pus formation but were not seen in other groups. Increased risk of infection in diabetic wounds could be explained by delayed wound healing and prolongation of all 4 phases of healing especially the inflammatory phase, thus impairing the immune function, and increases the susceptibility to infection and microbial invasion[45]. The primary cause of ongoing inflammatory condition in diabetic wound healing is impeded conversion of M1 to M2 macrophages. Persistence of M1 macrophages for prolonged period leads to release of tumor necrotic factor alpha (TNF-a) as well as interleukin 6 (IL-6), that severely damage the tissue[46,47]. Infection may also be due to poor vascular flow that mostly accompanies diabetic wounds which interferes with normal wound healing[35].

The reduced inflammation seen in PRP treatment groups (II, IV) could be expressed by the anti-inflammatory mediators found in PRP such as IL-17A and IL-1β[37]. This suggests that PRP has the ability to regulate wound inflammation, and hence leads to improvement of skin wound repair. Locally injected BM-MSCs have also been shown to attenuate wound inflammation by inhibiting inflammatory cell infiltration and by supressing the expression of proinflammatory cytokine production as CD45, IL-2 and matrix metalloproteinase 2 (MMP2)[48]. This may explain the least cardinal signs of inflammation that appeared in groups III and IV.

Scab (crust) formation was demonstrated in groups I, group II (PRP group) and in group III (stem cells group) at days 4 and 7 post surgery while in group IV no scab was formed. The goal of scab formation is to close the wound so that microbial agents and other foreign objects cannot enter, as well as to maintain humidity underneath the scab[49,50]. The scab will come off the incision once the new epidermis layer beneath it has fully developed because The growing tissue will stretch fibrin and push or breakdown collagen due to the enzymes released by leukocytes and epidermal cells[51]. The collagen and fibrin layer of the scab, however, can disrupt the migration of epidermal cells from skin appendages, slowing the process of re-epithelialization[49,50]. Thus, explaining the rapid wound closure in group IV when compared to the other 3 groups as no scab was noticed morphologically covering the wound.

Gross morphological examination on day 30 revealed complete closure of the wound in all study groups but with obvious scar formation, redness, and absence of hair in group I. Group II showed less prominent scar formation when compared to group I, whereas in groups III & IV showed well healed skin wounds with intact skin with no scar formation.

In addition to impeding wound healing, the loss or injury of skin appendages affects skin function and leads to scar formation as Weng *et al*.[52] demonstrated. This explains the bad obvious scar formed in group I.

Rosadi *et al*.[53] clarified that the use of PRP can improve collagen deposition as well as it effectively shorten healing time, and this minimizes the potential for scarring, which is necessary to get better tissue remodeling quality as Zeng *et al*.[54] mentioned.

Absence of scar formation and proper wound healing in the BM-MSCs treated groups (group III and IV) could be explained by decreased expression of certain factors as TGF-β1 and increased expression of others such as TGF-β3 through inhibiting the signal pathway of TGF-β/Smad which is an important pathogenic mechanism in wound repair[55]. Similar results were seen by Jiang *et al*.[56] who revealed that human bone marrow mesenchymal stem cell-derived exosomes (hBM-MSC-Ex) could improve healing of wounds by deactivating the signal pathway of TGF-β/Smad and hence decreased expression of TGF-β1 which is known to be a main factor in the scarring of tissues[57]. During wound repair, TGF-β3 possesses anti-fibrotic or scar-less properties and is crucial in controlling the migration of skin cells[58].

Other factors secreted by stem cells include fibroblast growth factor (bFGF) that shown to accelerate skin regeneration, as it remarkably alleviates scarring in healing of diabetic wound[59]. Chen *et al*.[60] reported that FGF produced from stem cells might hasten kinetics of wound repair in ulcers due to diabetes as it stimulates proliferation of fibroblasts. In addition, Li *et al*.[61] mentioned that MSCs - derived products , as exosomes, led to deposition of collagen and had antifibrotic role in hypertrophic scars.

Histological sections of the induced wound were examined on days 7, 14 and 30 of the study period to demonstrate the different stages of wound healing mentioned before. Light microscopic examination of groups I and II on day 7 showed disturbed epidermis with disorganized keratinocytes and areas of large fluid filled spaces, the wound bed showed massive inflammatory cells infiltration with congested blood vessels. No skin appendages were noted.

In this study, the results that were recorded in control group were in agreement with Kamar *et al*.[62] whose study revealed gross and histological delay of wound healing in the form of failure of wound closure, diffuse disfigurement of keratinocytes and defective collagen formation in the wound bed. These findings might be due to the ongoing inflammatory process in diabetic wounds leading to elevated inflammatory cytokines levels, which became destructive and promoted apoptosis in the diabetic wounds as Amer *et al*.[63] mentioned in their study. Aryan *et al*.[64] also found on days 7, 15, and 28 after surgery an increase in inflammatory cells number in the control group of their study that goes in line with the present results.

Increased number of myofibroblasts was identified in group II. The TGF-β pathway's modification resulted in the accumulation of myofibroblasts[65]. Moreover, prior research indicated that increased number of myofibroblasts at the wound site was as a result of using PRP to promote wound healing and this was assessed by measuring the quantity of alpha smooth muscle actin (α –SMA) which particularly myofibroblasts express[66]. The contraction of wounds is thought to be significantly influenced by myofibroblasts. The granulation tissue formation and the steady increase in the differentiation of fibroblasts into myofibroblasts are what will actually cause the wound margin to contract[67,68].

The epidermis improved in groups III and IV, but it was thicker and more organized in group IV, moreover there was a decrease in invasion of inflammatory cells as well as congested blood vessels in both groups, few regenerating sebaceous glands and hair follicles with newly formed blood vessels were seen in group IV and increased number of mast cells in group III was detected.

Aryan *et al*.[64] mentioned that MSCs produce a lot of elements that are crucial in the normal function of the cell during the culturing process. They suggest that the hBM-MSCs release several factors, as anti-inflammatory cytokines that explains the reduced inflammation in groups III & IV.

Additionally, Aryan *et al*.[64] demonstrated that healing with granular tissue formation and thick dermis was observed in human bone marrow mesenchymal stem cell conditioned medium group (hBM-MSC-CM). They added that on days 7 and 14 of their study, there was a notable rise in fibroblast cells in the hBM-MSC-CM group, suggesting that the hBM-MSC-CM groups began the proliferation phase sooner. The findings offer compelling proof that some factors (bFGF) within the hBM-MSC-CM group could stimulate fibroblasts, keratinocytes, and cell proliferation, leading to enhanced granulation tissue development in the process of wound healing.

The observed increase in mast cells in group III in this study was in agreement with Da Costa *et al*.[69] who found less mast cells in diabetic mice skin and increase in the mast cells (MCs) count after MSC administration. MCs occupy about 8% of cell count within the dermis, and they are essential for wound healing[70]. This may explain the improved healing of the skin wounds in groups III and IV.

On day 14, histological examination of the induced wound to assess proliferation and regeneration was performed. Complete thick regenerated epidermis which is covered by keratin with increased keratohyaline granules were noticed in groups IV, the reappearance of keratohyaline granules indicates restoration of the full functional epidermis, least inflammatory cell infiltrate, increased newly formed blood vessels, increased number of fibroblast cells and regenerated hair follicles were identified in the dermis of group IV compared to other study groups. Group I showed thin, disorganized epidermis and increased inflammatory cell infiltrate as well as few blood vessels were seen in the dermis with absence of skin appendages in groups I and II.

Diabetes impairs the angiogenesis process in healing of wounds. Diabetic wounds affected by inadequate angiogenesis reveal reduced vascularity. Diabetes causes a marked inhibition of wound healing that leads to chronic non-healing wounds. A lot of studies have revealed a link between poor angiogenesis and the pathologic wound healing found in diabetes patients[35].

The decline in formation of blood vessels in group I in the present work may be explained by alterations in factors responsible for capillary maturation and anti-angiogenic elements in wounds, in addition to the reduction in vascular endothelial growth factor (VEGF) which is a factor that promotes angiogenesis. Studies on diabetic wound healing have examined the production of the pigment epithelium derived factor (PEDF) which is an anti-angiogenic element and it was discovered that individuals with diabetic foot ulcers had greater circulating levels of PEDF[35].

Diabetes naturally reduces the number of endothelial progenitor cells (EPCs) that are derived from bone marrow, moreover, it alters the secretion of vascular maturation and pro-angiogenic factors[71]. Consequently, diabetic tissues have less baseline vascularity due to this deficiency, which probably has an impact on wound angiogenesis[72].Delayed wound healing in diabetic control group may also be explained by decrease of fibroblast cells that led to slow proliferation rate[73].

Groups II, IV revealed more rapid wound healing and significant improvement in wound closure relative to the control group and this could be related to the growth factors accumulated in the platelet granules as Amer *et al*.[63] said. These factors include VEGF, which promotes angiogenesis, PDGF, and TGF-β[74]. This was in line with Rezende *et al*.[75] who observed decrease in the size of the wound in the PRP treated wounds after 14 and 21 days in relation to the groups that were not treated .

The results of group II in this study matched with Wang *et al*.[76] who mentioned that PRP enhanced angiogenesis in open wounds as it led to production of large quantities of VEGF, which is thought to be the primary growth factor that is involved in the process of angiogenesis. VEGF has a paracrine action on TGF-β during wound healing to help in the regeneration of blood vessels in the wound site[77]. Furthermore, the study results of Hui *et al*.[78] confirm that TGF-β and VEGF-α work in concert to promote vascular regeneration. Moreover, FGF and PDGF which are produced by PRP chemoattract smooth muscle cells that leads to growth of smooth muscle cell and vessel enlargement[77]. Badis and Omar[79] stated that the neovascularization that occurs during skin wounds encourages the infiltration of inflammatory cells that serve to debride the lesional focus which explains the increase of inflammatory cells that were noted in this study.

Moreover, MSCs secrete growth factors including VEGF, bFGF, and keratinocyte growth factor (KGF) throughout the proliferative and remodeling phase; these factors encourage granulation and neovascularization[80]. Park *et al*.[59] added that epidermal growth factor (EGF), KGF, and bFGF are well-known secretory factors that can encourage the skin cells' migration and proliferation, including keratinocytes, dermal fibroblasts, and vascular endothelial cells which explains the increased number of blood vessels with improvement of angiogenesis process that were observed in groups III and IV.

Yao *et al*.[48] demonstrated that some studies have stated that MSCs improve wound healing because of MSCs differentiation but other people have mentioned that the good effects of MSCs may be exerted by reducing inflammation instead of differentiating.

In this study, regenerated skin appendages were noted in groups III and IV obviously at days 14 and 30 of the study that agreed with Feng *et al*.[81] who demonstrated an increase in the hair follicles number after injection of adipose -derived stem cells intradermally (ASCs). They confirmed that ASCs accelerated appendage progenitor cells proliferation and differentiation through secretion of growth factors. Additionally, Duan *et al*.[82] reported that the skin in the epidermal stem cell-derived exosomes group (EPSC-Exos) had more appendages than other study groups.

On day 30, histological examination of the wound areas concurred with the gross morphological results. Group IV showed best healing with regenerated well-formed complete epidermis covered by keratin containing abundant keratohyaline granules followed by group III. Moderate complete regenerated blood vessels were seen in the dermis with complete regenerated well developed hair follicles and sebaceous glands in comparison to the other study groups. There was absence of skin appendages in groups I, II and increased inflammatory cells in group I.

Re-epithelialization is the process by which epidermal cells proliferate and differentiate. Numerous growth factors, including epidermal growth factor (EGF), FGF, VEGF, TGF -β, PDGF, as well as IGF-1, are important in this process[37]. The process of re-epithelialization may be impacted by the blockage of extracellular matrix (ECM) formation[83]. Keratinocytes move through a temporary matrix made of type I collagen as the wound first starts to heal. Matrix metalloproteinases (MMPs) as well as tissue inhibitor of metalloproteinases (TIMPs) must coexist in harmony for this process to occur. While the gene for TIMPs is silenced in diabetic wounds, MMP expression is elevated, which intensifies collagen breakdown and prevents re-epithelialization as Chang and Nguyen said[84]. This explains the deterioration in the repair of skin wound in group I.

The above results agreed with Xu *et al*.[37] who reported that PRP enhanced re-epithelialization by increasing IGF-1 production in wound tissue. It was mentioned that PRP can stimulate tissue cells to secrete the growth factors by exerting autocrine or paracrine activities. TGF-β. EGF and IGF-1 has been shown to be some of these factors that are crucial for the regeneration and repair of skin tissues. According to certain research, PRP may increase IGF-1 expression in injuries such osteoarthritis and nerve damage[85,86].

Additionally PRP could significantly enhance migration of epidermal stem cells (ESCs)[37]. ESCs are essential for effective reepithelialization and perform critical functions in differentiation and proliferation of epidermal cells[44]. When a wound develops, ESCs rapidly replicate at the wound's base, grow to the center of wound, and gradually differentiate into daughter cells to repair the defect of skin tissue[37].

Improved healing seen in the form of well-developed thick regenerated epithelium seen in groups III and IV is explained by epithelial differentiation and secretion by MSCs. Park *et al*.[59] reported that a number of tissue repair regulators as growth factors, cytokines, as well as chemokines as bFGF, EGF, hepatocyte growth factor (HGF), and TGF-β, have been reported to be secreted by stem cells produced from different tissues. Increased levels of three factors (HGF, EGF, and bFGF) were found in secretome of stem cell. These secretory substances dramatically increased wound reepithelialization and encouraged keratinocyte migration in *vivo*.

You and Nam[87] mentioned that EGF- secreting stem cells hasten wound healing by promoting migration and proliferation of fibroblast. Also, HGF has been demonstrated to have anti-apoptotic and mitogenic actions on epithelial and endothelial cells[59].

As a result, on the level of histological evaluation, the combined treated group IV showed the best results. This might be clarified by the synergistic healing effect of growth factors of PRP and BM-MSCs. Group IV showed the best results regarding the timing of complete wound healing in relation to other research groups as proteins, growth factors, and enzymes that enhance MSC efficacy of wound healing are released from PRP[8].

Additionally, using MSCs and PRP in combination with each other is more effective in enhancing vascularization and tissue regeneration compared to using PRP or MSCs alone. Furthermore, PRP acts as an adjuvant to boost the engrafted MSCs' therapeutic efficacy, as well as to increase their adaptability and persistence at the site of the wound. It also serves as a cytoprotectant that prevents oxidative damage of MSCs by improving ATP-linked respiration and consumption of oxygen[8].

Regarding the results of Masson's trichrome staining, on the 7th day, the dermis showed fine pale collagen fibers arranged in one direction in groups I, II. The amount of collagen fibers increased significantly in group III, while group IV showed dense collagen strands are deposited moderately running in different directions. The amount

of collagen increased at day 14 in the study groups, but the greatest amount was observed in groups III and IV and the collagen fibers were thick and running in different directions. Collagen bundles were most organized and well developed in group IV. On day 30, it was observed a massive increase in dense collagen bundle deposition running in different directions in groups III, IV in comparison with groups I, II in which there was less amount of collagen running in one direction.

A crucial stage in wound healing is the organized and sufficient deposition of collagen. The wound's matrix composition changes over time: Initially, fibrin and fibronectin make up the majority of the provisional ECM. The granulation tissue, which is primarily made of fibronectin, replaces the provisional ECM in the proliferative phase, creates a scaffold for the following deposition of collagen types I and III[88].

Deficient fibroblast proliferation in the dermis due to diabetes mellitus may be linked to the observed deficient collagen fibers creation in the control group. This may be explained as high glucose environment inhibits M1 to M2 macrophage transformation, which lowers myofibroblast counts, results in insufficient collagen release, and delays wound contraction[89], and this was in agreement with Amer *et al*.[63] Myofibroblast plays a very important role in producing collagen and generating extracellular matrix (ECM) during the proliferative stage of wound healing[90].

Accordingly, Tan *et al*.[91] reported that a variety of proteases were active in diabetic wounds, readily breaking down growth factors in the area of the wound and causing a malfunction in the process of recovery of diabetic skin ulcers.

The results regarding group II revealed increase in the amount of collagen and improvement in its distribution at day 14 and day 30 relative to group I. This can be explained by that the PRP required additional time to encourage granulation tissue maturation that aligned with the findings of Farghali *et al*.[92].

In the present work, largest amount and best organised collagen bundles were observed in groups III and IV. It has been previously demonstrated that Mesenchymal stem cells can stimulate collagen synthesis and promote fibroblast proliferation and hence enhance wound healing by directly secreting many factors as TGF-β and bFGF. (64) In addition, Hsu *et al*.[93] claimed that, MSCs derived exosomes could increase the amount of TGF-β secreted by monocytes or macrophages in the wound area. TGF-β enhances the growth of fibroblasts by triggering the signaling pathway of TGF-β /Smad3 and increases the synthesis of type I collagen. When TGF-β binds to fibroblast receptors, Smad3 complex is activated promoting nuclear transcription and initiating the production of collagen[94].

Regarding the immunohistochemical results, a statistically significant decrease in number of infiltrating CD68 macrophages was observed in group IV compared to other studied groups. Also group III showed statistically significant decrease in infiltrating CD68 macrophages number in comparison to groups I, II and there was statistically significant decrease in number of these cells in group II relative to group I at days 7, 14 and 30 of the study period.

Moreover, the number of infiltrating CD68 macrophages declined in all studied groups at day 30 in comparison to day 14, and day 7. This may be explained as the macrophages' infiltration increases in the inflammatory stage of the healing of wound that was assessed on day 7 and decreases during the proliferative phase which was assessed on day 14 and it decreased much more during the remodeling stage of wound healing that was assessed on day 30 post wound formation.

The above results agreed with Miao *et al*.[6] who documented that the number of CD68 macrophages increased significantly in both normal and diabetic groups and reached the peak on day 3, then decreased on day 13. They added that the quantity of CD68 cells was higher on day 3 in the normal nondiabetic group, but lower at day 7 than in the diabetic group which proves that diabetes prolongs the inflammatory stage and delays the proliferative stage of healing of wounds.

Macrophages show up in the wound 48 to 72 hours post injury and regulate proliferation. There are two types of wound-associated macrophages: classically activated M1 macrophages as well as alternatively activated M2 macrophages, and by day 2 there are about 3000 cells in each wound[95]. This is stable for the first five days before progressively declining to stable values by day 14[96]. In the initial phase of inflammation, M1 macrophages are drawn to the area of the wound and release proinflammatory cytokines like IL-6, TNF- α, and other elements that speed up the beginning phases of wound healing[97]. These cells are in charge of angiogenesis and production of collagen in the wound during the late stages of the inflammatory response[95].

Lei *et al*.[95] mentioned in their study that there was a prominent decrease in macrophages count in the PRP treated groups on 7th day of their study which agreed with the results in this study and this may be due to microparticles in PRP that cause apoptosis., that have the ability to convert monocytes to M2 macrophages. Moreover, platelet microparticles are able to decrease the release of TNF-α and decrease production of CD40L, that attaches to CD40 on the macrophages to activate inflammatory processes[98].

The results in this work were in line with Yao *et al*.[48] as they said that MSCs treatment decreases inflammatory cells and CD68 macrophages infiltration, MSCs inhibit infiltration of macrophages maybe by decreasing the production of the macrophage inflammatory protein-1alpha (MIP-1a).

The results of this research matched with that of Aryan *et al*.[64] who showed significant decrease in macrophages

and neutrophils numbers in hBM-MSC-CM group. This might be due to its various factors, that can resolve and decrease the phase of inflammation and activate proliferative phase; thus, by secreting several factors like granulocyte/macrophage colony-stimulating factor (GM-CSF) in the wounded area.

Moreover, it was demonstrated in previous study that MSCs released an enormous quantity of HGF hat was highly expressed after its application. It leads to down-regulation in expression of monocyte chemoattractant protein 1 (MCP-1) expression, thus reducing macrophages infiltration in diabetic tissue[99].

Using MSCs has been shown to either decrease macrophage infiltration in the target tissue in several animal models or flip macrophages to the alternative M2 type, which contributes to homeostasis of tissues as well as it primarily secretes anti-inflammatory cytokines during the repair phase[99].

The above results were in contrast with Park *et al*.[59] as they demonstrated that there was extensive rise in CD68 macrophages cell numbers in wounds treated by stem cell secretome in comparison with the control groups. This may be explained by the stimulating signaling of PI3K/Akt or FAK/ERK1/2 by stem cell secretome leading to increase in dermal cellular components migration and proliferation throughout the repair of tissues.

CONCLUSION

The best healing results were seen in group IV(PRP + stem cells group) followed by group III (stem cells group) and group II (PRP group) relative to group I (control group). In this study, the results showed a synergistic effect of the combination between BM-MSCs and PRP on STZ-induced diabetic cutaneous wounds. As this combination promoted wound closure progress and healing by activation of surface re-epithelization, differentiation, and improving angiogenesis. So this combination might be used as a new approach to the treatment of foot ulcers in diabetics to decrease the progress of gangrene and accelerate wound healing.

CONFLICT OF INTERESTS

There are no conflicts of interest.

REFERENCES

1. Chicharro-Alcántara D, Rubio-Zaragoza M, Damiá-Giménez E, Carrillo-Poveda JM, Cuervo-Serrato B, Peláez-Gorrea P, *et al*. Platelet rich plasma: new insights for cutaneous wound healing management. J Funct Biomater 2018;9(1):10. DOI:10.3390/jfb9010010.
2. Heller AJ. Allergic skin disease. Facial Plast Surg Clin North Am 2012;20(1):31-42. DOI:10.1016/j.fsc.2011.10.004.
3. Ross MH, Pawlina W. Histology : a text and atlas : with correlated cell and molecular biology. Seventh ed. Philadelphia: Wolters Kluwer; 2016. ISPN:9781469889313.
4. Wilgus TA, Wulff BC. The importance of mast cells in dermal scarring. ADV wound care 2014;3(4):356-65. DOI:10.1089/wound.2013.0457.
5. Teng M, Huang Y, Zhang H. Application of stems cells in wound healing—an update. Wound Repair Regen 2014;22(2):151-60. DOI:10.1111/wrr.12152.
6. Miao M, Niu Y, Xie T, Yuan B, Qing C, Lu S. Diabetes-impaired wound healing and altered macrophage activation: A possible pathophysiologic correlation. Wound Repair Regen 2012;20(2):203-13. DOI:10.1111/j.1524-475X.2012.00772.x.
7. Yan J, Tie G, Wang S, Tutto A, DeMarco N, Khair L, *et al*. Diabetes impairs wound healing by Dnmt1-dependent dysregulation of hematopoietic stem cells differentiation towards macrophages. Nat Commun 2018;9(1):33. DOI:10.1038/s41467-017-02425-z.
8. Hersant B, Sid-Ahmed M, Braud L, Jourdan M, Baba-Amer Y, Meningaud J-P, *et al*. Platelet-Rich Plasma Improves the Wound Healing Potential of Mesenchymal Stem Cells through Paracrine and Metabolism Alterations. Stem Cells Int 2019;2019:1-14. DOI:10.1155/2019/1234263.
9. Zhang C, Zhu Y, Lu S, Zhong W, Wang Y, Chai Y. Platelet-rich plasma with endothelial progenitor cells accelerates diabetic wound healing in rats by upregulating the Notch1 signaling pathway. J Diabetes Res 2019;2019:5920676. DOI:10.1155/2019/5920676.
10. Lim JZM, Ng NSL, Thomas C. Prevention and treatment of diabetic foot ulcers. J R Soc Med 2017;110(3):104-9. DOI:10.1177/0141076816688346.
11. Jee C-H, Eom N-Y, Jang H-M, Jung H-W, Choi E-S, Won J-H, *et al*. Effect of autologous platelet-rich plasma application on cutaneous wound healing in dogs. J Vet Sci 2016;17(1):79-87. DOI:10.4142/jvs.2016.17.1.79.
12. El-Aassar M, Ibrahim OM, Fouda MM, Fakhry H, Ajarem J, Maodaa SN, *et al*. Wound dressing of chitosan-based-crosslinked gelatin/polyvinyl pyrrolidone embedded silver nanoparticles, for targeting multidrug resistance microbes. Carbohydrate Polymers 2021;255:117484. DOI:10.1016/j.carbpol.2020.117484.
13. Fouda MM, Abdel-Mohsen A, Ebaid H, Hassan I, Al-Tamimi J, Abdel-Rahman RM, *et al*. Wound healing of different molecular weight of hyaluronan; in-*vivo* study. Int J Biol Macromol 2016;89:582-91. DOI:10.1016/j.ijbiomac.2016.05.021.
14. Lopes L, Setia O, Aurshina A, Liu S, Hu H, Isaji T, *et al*. Stem cell therapy for diabetic foot ulcers: a review of preclinical and clinical research. Stem Cell Res Ther 2018;9(1):188. DOI:10.1186/s13287-018-0938-6.

15. Reddy SHR, Reddy R, Babu NC, Ashok G. Stem-cell therapy and platelet-rich plasma in regenerative medicines: a review on pros and cons of the technologies. J Oral Maxillofac Pathol 2018;22(3):367-74. DOI:10.4103/jomfp.JOMFP_93_18.

16. Chen P, Huang L, Ma Y, Zhang D, Zhang X, Zhou J, *et al*. Intra-articular platelet-rich plasma injection for knee osteoarthritis: a summary of meta-analyses. J Orthop Surg Res 2019;14(1):385. DOI:10.1186/s13018-019-1363-y.

17. Mahmoudian-Sani MR, Rafeei F, Amini R, Saidijam M. The effect of mesenchymal stem cells combined with platelet-rich plasma on skin wound healing. J Cosmet Dermatol 2018;17(5):650-9. DOI:10.1111/jocd.12512.

18. Zaminy A, Shokrgozar MA, Sadeghi Y, Noroozian M, Heidari MH, Piryaei A. Transplantation of schwann cells differentiated from adipose stem cells improves functional recovery in rat spinal cord injury. Arch Iran Med 2013;16(9):533-41.DOI: 013169/aim.0011.

19. Lian Z, Yin X, Li H, Jia L, He X, Yan Y, *et al*. Synergistic Effect of Bone Marrow-Derived Mesenchymal Stem Cells and Platelet-Rich Plasma in Streptozotocin-Induced Diabetic Rats. Ann Dermatol 2014;26(1):1-10. DOI:10.5021/ad.2014.26.1.1.

20. Mehanna RA, Nabil I, Attia N, Bary AA, Razek KA, Ahmed TA, *et al*. The effect of bone marrow-derived mesenchymal stem cells and their conditioned media topically delivered in fibrin glue on chronic wound healing in rats. Biomed Res Int 2015;2015:846062. DOI:10.1155/2015/846062.

21. El Sadik AO, El Ghamrawy TA, Abd El-Galil TI. The effect of mesenchymal stem cells and chitosan gel on full thickness skin wound healing in albino rats: histological, immunohistochemical and fluorescent study. PloS one 2015;10(9):e0137544. DOI:10.1371/journal.pone.0137544.

22. Argôlo Neto NM, Del Carlo RJ, Monteiro BS, Nardi NB, Chagastelles PC, de Brito AFS, *et al*. Role of autologous mesenchymal stem cells associated with platelet-rich plasma on healing of cutaneous wounds in diabetic mice. Clin Exper Dermatol 2012;37(5):544-53. DOI:10.1111/j.1365-2230.2011.04304.x.

23. Aydin O, Karaca G, Pehlivanli F, Altunkaya C, Uzun H, Özden H, *et al*. Platelet-rich plasma may offer a new hope in suppressed wound healing when compared to mesenchymal stem cells. J Clin Med 2018;7(6):143. DOI:10.3390/jcm7060143.

24. Zakaria DM, Zahran NM, Arafa SAA, Mehanna RA, Abdel-Moneim RA. Histological and physiological studies of the effect of bone marrow-derived mesenchymal stem cells on bleomycin induced lung fibrosis in adult albino rats. Tissue Eng Regen Med 2021;18(1):127-41.DOI:10.1007/s13770-020-00294-0.

25. Edalatmanesh M-A, Matin MM, Neshati Z, Bahrami A-R, Kheirabadi M. Systemic transplantation of mesenchymal stem cells can reduce cognitive and motor deficits in rats with unilateral lesions of the neostriatum. Neurol Res 2010;32(2):166-72. DOI:10.1179/174313209X409025.

26. Baghaei K, Hashemi SM, Tokhanbigli S, Rad AA, Assadzadeh-Aghdaei H, Sharifian A, *et al*. Isolation, differentiation, and characterization of mesenchymal stem cells from human bone marrow. Gastroenterol Hepatol Bed Bench 2017;10(3):208–13. DOI:10.22037/ghfbb.v0i0.1089.

27. Dhurat R, Sukesh M. Principles and Methods of Preparation of Platelet-Rich Plasma: A Review and Author's Perspective. J Cutan Aesthet Surg 2014;7(4):189-97. DOI:10.4103/0974-2077.150734.

28. Kaur M, Bedi O, Sachdeva S, Reddy BK, Kumar P. Rodent animal models: from mild to advanced stages of diabetic nephropathy. Inflammopharmacology 2014;22(5):279-93. DOI:10.1007/s10787-014-0215-y.

29. Dogan S, Demirer S, Kepenekci I, Erkek B, Kiziltay A, Hasirci N, *et al*. Epidermal growth factor-containing wound closure enhances wound healing in non-diabetic and diabetic rats. Int Wound J 2009;6(2):107-15. DOI:10.1111/j.1742-481X.2009.00584.x.

30. Ebrahim N, Dessouky A, Mostafa O, Yousef M, Seleem Y, El Gebaly E, *et al*. Adipose Mesenchymal Stem Cells Combined with Platelet Rich Plasma Accelerate Diabetic Wound Healing by Modulating Notch Pathway. Stem Cell Res Ther 2021;12(1):392. DOI:10.1186/s13287-021-02454-y.

31. Kirkpatrick LA, Feeney BC. A Simple Guide to IBM SPSS Statistics for Version 22.0. Student ed. Belmont, Calif: Wadsworth, Cengage Learning; 2014. DOI:10.5555/2692437.

32. Kotz S, Balakrishnan N, Read CB, Vidakovic B. Encyclopedia of Statistical Sciences. 2nd ed. Hoboken, N.J: Wiley-Interscience; 2006. DOI:10.1002/0471667196.

33. Harries RL, Bosanquet DC, Harding KG. Wound bed preparation: TIME for an update. Int Wound J 2016;13(S3):8-14. DOI:10.1111/iwj.12662.

34. Dreifke MB, Jayasuriya AA, Jayasuriya AC. Current wound healing procedures and potential care. Mater Sci Eng C Mater Biol Appl 2015;48:651-62. DOI:10.1016/j.msec.2014.12.068.

35. Okonkwo UA, DiPietro LA. Diabetes and wound angiogenesis. Int J Mol Sci 2017;18(7):1419. DOI:10.3390/ijms18071419.

36. Lv Q, Deng J, Chen Y, Wang Y, Liu B, Liu J. Engineered Human Adipose Stem-Cell-Derived Exosomes Loaded with miR-21-5p to Promote Diabetic Cutaneous Wound Healing. Mol Pharm 2020;17(5):1723-33. DOI:10.1021/acs.molpharmaceut.0c00177.

37. Xu P, Wu Y, Zhou L, Yang Z, Zhang X, Hu X, *et al*. Platelet-rich plasma accelerates skin wound healing by promoting re-epithelialization. Burns Trauma 2020;8:tkaa028. DOI:10.1093/burnst/tkaa028.
38. Yong KW, Choi JR, Mohammadi M, Mitha AP, Sanati-Nezhad A, Sen A. Mesenchymal stem cell therapy for ischemic tissues. Stem Cells Int 2018;2018:8179075. DOI:10.1155/2018/8179075.
39. Leonardi D, Oberdoerfer D, Fernandes MC, Meurer RT, Pereira-Filho GA, Cruz P, *et al*. Mesenchymal stem cells combined with an artificial dermal substitute improve repair in full-thickness skin wounds. Burns 2012;38(8):1143-50. DOI:10.1016/j.burns.2012.07.028.
40. Hu M, Ludlow D, Alexander JS, McLarty J, Lian T. Improved wound healing of postischemic cutaneous flaps with the use of bone marrow-derived stem cells. Laryngoscope 2014;124(3):642-8. DOI:10.1002/lary.24293.
41. Bryda EC. The Mighty Mouse: the impact of rodents on advances in biomedical research. Mo Med 2013;110(3):207-11. PMID: 23829104; PMCID: PMC3987984.
42. Čriepoková Z, Lenhardt L, Gál P. Basic Roles of Sex Steroid Hormones in Wound Repair with Focus on Estrogens (A Review). Folia Veter 2016;60(1):41-6. DOI:10.1515/fv-2016-0006.
43. Furman BL. Streptozotocin-Induced Diabetic Models in Mice and Rats. Curr Protoc 2021;1(4):e78. DOI:10.1002/cpz1.78.
44. Li Y, Zhang J, Yue J, Gou X, Wu X. Epidermal stem cells in skin wound healing. ADV wound care 2017;6(9):297-307. DOI:10.1089/wound.2017.0728.
45. Noor S, Zubair M, Ahmad J. Diabetic foot ulcer—a review on pathophysiology, classification and microbial etiology. Diabetes Metab Syndr 2015;9(3):192-9. DOI:10.1016/j.dsx.2015.04.007.
46. Louiselle AE, Niemiec SM, Zgheib C, Liechty KW. Macrophage polarization and diabetic wound healing. Transl Res 2021;236:109-16. DOI:10.1016/j.trsl.2021.05.006.
47. Wolf SJ, Melvin WJ, Gallagher K. Macrophage-mediated inflammation in diabetic wound repair. Semin Cell Dev Biol 2021;119:111-8. DOI:10.1016/j.semcdb.2021.06.013.
48. Yao L, Li Z-r, Su W-r, Li Y-p, Lin M-l, Zhang W-x, *et al*. Role of mesenchymal stem cells on cornea wound healing induced by acute alkali burn. PloS one 2012;7(2):e30842. DOI:10.1371/journal.pone.0030842.
49. Ribeiro AM, Flores-Sahagun TH. Application of stimulus-sensitive polymers in wound healing formulation. Int J Pol Mater Poly Biomater 2020;69(15):979-89. DOI:10.1080/00914037.2019.1655744.
50. Abdelhak M. A review: Application of biopolymers in the pharmaceutical formulation. J Adv Bio-Pharm Pharmacovigil 2019;1(1):15-25. DOI:10.5281/zenodo.2577643.
51. Panayi AC, Reitblat C, Orgill DP. Wound healing and scarring. In: Ogawa R, (ed). Total Scar Management: From Lasers to Surgery for Scars, Keloids, and Scar Contractures. Singapore: Springer Nature; 2020. 3-16. DOI:10.1007/978-981-32-9791-3.
52. Weng T, Wu P, Zhang W, Zheng Y, Li Q, Jin R, *et al*. Regeneration of skin appendages and nerves: current status and further challenges. J Transl Med 2020;18(1):53. DOI:10.1186/s12967-020-02248-5.
53. Rosadi I, Karina K, Rosliana I, Sobariah S, Afini I, Widyastuti T, *et al*. In *vitro* study of cartilage tissue engineering using human adipose-derived stem cells induced by platelet-rich plasma and cultured on silk fibroin scaffold. Stem Cell Res Ther 2019;10(1):1-15. DOI:10.1186/s13287-019-1443-2.
54. Zeng X-L, Sun L, Zheng H-Q, Wang G-L, Du Y-H, Lv X-F, *et al*. Smooth muscle-specific TMEM16A expression protects against angiotensin II-induced cerebrovascular remodeling via suppressing extracellular matrix deposition. J Mol Cell Cardiol 2019;134:131-43. DOI:10.1016/j.yjmcc.2019.07.002.
55. Hu H-H, Chen D-Q, Wang Y-N, Feng Y-L, Cao G, Vaziri ND, *et al*. New insights into TGF-β/Smad signaling in tissue fibrosis. Chem Biol Interact 2018;292:76-83. DOI:10.1016/j.cbi.2018.07.008.
56. Jiang T, Wang Z, Sun J. Human bone marrow mesenchymal stem cell-derived exosomes stimulate cutaneous wound healing mediates through TGF-β/Smad signaling pathway. Stem Cell Res Ther 2020;11(1):198. DOI:10.1186/s13287-020-01723-6.
57. Mokoena D, Kumar SSD, Houreld NN, Abrahamse H. Role of photobiomodulation on the activation of the Smad pathway via TGF-β in wound healing. J Photochem Photobiol B 2018;189:138-44. DOI:10.1016/j.jphotobiol.2018.10.011.
58. Lichtman MK, Otero-Vinas M, Falanga V. Transforming growth factor beta (TGF-β) isoforms in wound healing and fibrosis. Wound Repair Regen 2016;24(2):215-22. DOI:10.1111/wrr.12398.
59. Park S-R, Kim J-W, Jun H-S, Roh JY, Lee H-Y, Hong I-S. Stem cell secretome and its effect on cellular mechanisms relevant to wound healing. Mol Ther 2018;26(2):606-17. DOI:10.1016/j.ymthe.2017.09.023.
60. Chen S, Shi J, Zhang M, Chen Y, Wang X, Zhang L, *et al*. Mesenchymal stem cell-laden anti-inflammatory hydrogel enhances diabetic wound healing. Sci Rep 2015;5(1):18104. DOI:10.1038/srep18104.

61. Li Y, Zhang J, Shi J, Liu K, Wang X, Jia Y, *et al*. Exosomes derived from human adipose mesenchymal stem cells attenuate hypertrophic scar fibrosis by miR-192-5p/IL-17RA/Smad axis. Stem Cell Res Ther 2021;12:221. DOI:10.1186/s13287-021-02290-0.
62. Kamar SS, Abdel-Kader DH, Rashed LA. Beneficial effect of Curcumin Nanoparticles-Hydrogel on excisional skin wound healing in type-I diabetic rat: Histological and immunohistochemical studies. Ann Anat 2019;222:94-102. DOI:10.1016/j.aanat.2018.11.005.
63. Amer SM, Ali SM, Elmarakby D, Abdallah H. Histological study on the effect of insulin and platelet-rich plasma on skin wounds induced in diabetic adult male albino rats. Egypt J Histol 2021;46(1):263-79. DOI:10.21608/EJH.2021.86084.1527.
64. Aryan A, Bayat M, Bonakdar S, Taheri S, Haghparast N, Bagheri M, *et al*. Human bone marrow mesenchymal stem cell conditioned medium promotes wound healing in deep second-degree burns in male rats. Cells Tissues Organs 2019;206(6):317-29. DOI:10.1159/000501651.
65. Koulikovska M, Szymanowski O, Lagali N, Fagerholm P. Platelet-rich plasma prolongs myofibroblast accumulation in corneal stroma with incisional wound. Curr Eye Res 2015;40(11):1102-10. DOI:10.3109/02713683.2014.978478.
66. Xiang Z, Zhou Q, Hu M, Sanders YY. MeCP2 epigenetically regulates alpha-smooth muscle actin in human lung fibroblasts. J Cell Biochem 2020;121(7):3616-25. DOI:10.1002/jcb.29655.
67. Hinz B, McCulloch CA, Coelho NM. Mechanical regulation of myofibroblast phenoconversion and collagen contraction. Exp Cell Res 2019;379(1):119-28. DOI:10.1016/j.yexcr.2019.03.027.
68. Ribatti D, Tamma R. Giulio Gabbiani and the discovery of myofibroblasts. Inflamm Res 2019;68:241-5. DOI:10.1007/s00011-018-01211-x.
69. da Costa Manso GM, Elias-Oliveira J, Guimarães JB, Pereira ÍS, Rodrigues VF, Burger B, *et al*. Xenogeneic mesenchymal stem cell biocurative improves skin wounds healing in diabetic mice by increasing mast cells and the regenerative profile. Regen Ther 2023;22:79-89. DOI:10.1016/j.reth.2022.12.006.
70. Ahmadi H, Bayat M, Amini A, Mostafavinia A, Ebrahimpour-Malekshah R, Gazor R, *et al*. Impact of preconditioned diabetic stem cells and photobiomodulation on quantity and degranulation of mast cells in a delayed healing wound simulation in type one diabetic rats. Lasers Med Sci 2022;37(3):1593-604. DOI:10.1007/s10103-021-03408-9.
71. Drela E, Stankowska K, Kulwas A, Rosc D. Endothelial progenitor cells in diabetic foot syndrome. Adv Clin Exp Med 2012;21(2):249-54. PMID: 23214290.
72. Kolluru GK, Bir SC, Kevil CG. Endothelial dysfunction and diabetes: effects on angiogenesis, vascular remodeling, and wound healing. Int J Vasc Med 2012;2012:918267. DOI:10.1155/2012/918267.
73. Abedin-Do A, Zhang Z, Douville Y, Méthot M, Rouabhia M. Effect of electrical stimulation on diabetic human skin fibroblast growth and the secretion of cytokines and growth factors involved in wound healing. Biology 2021;10(7):641. DOI:10.3390/biology10070641.
74. Golebiewska EM, Poole AW. Platelet secretion: From haemostasis to wound healing and beyond. Blood Rev 2015;29(3):153-62. DOI:10.1016/j.blre.2014.10.003.
75. Rezende RSd, Eurides D, Alves EGL, Venturini GC, Felipe RLd. Co-treatment of wounds in rabbit skin with equine platelet-rich plasma and a commercial ointment accelerates healing. Ciênc anim bras 2020;21:e–56274. DOI:10.1590/1809-6891v21e-56274.
76. Wang B, Geng Q, Hu J, Shao J, Ruan J, Zheng J. Platelet-rich plasma reduces skin flap inflammatory cells infiltration and improves survival rates through induction of angiogenesis: An experiment in rabbits. J Plast Surg Hand Surg 2016;50(4):239-45. DOI:10.3109/2000656X.2016.1159216.
77. Farghali HA, AbdElKader NA, AbuBakr HO, Aljuaydi SH, Khattab MS, Elhelw R, *et al*. Antimicrobial action of autologous platelet-rich plasma on MRSA-infected skin wounds in dogs. Sci Rep 2019;9(1):12722. DOI:10.1038/s41598-019-48657-5.
78. Hui Q, Chang P, Guo B, Zhang Y, Tao K. The clinical efficacy of autologous platelet-rich plasma combined with ultra-pulsed fractional CO2 laser therapy for facial rejuvenation. Rejuvenation Res 2017;20(1):25-31. DOI:10.1089/rej.2016.1823.
79. Badis D, Omar B. The effectiveness of platelet-rich plasma on the skin wound healing process: A comparative experimental study in sheep. Vet World 2018;11(6):800-8. DOI:10.14202/vetworld.2018.800-808.
80. Verma R, Kumar S, Garg P, Verma YK. Platelet-rich plasma: A comparative and economical therapy for wound healing and tissue regeneration. Cell Tissue Bank 2023;24(2):285-306. DOI:10.1007/s10561-022-10039-z.
81. Feng C-J, Lin C-H, Tsai C-H, Yang I-C, Ma H. Adipose-derived stem cells-induced burn wound healing and regeneration of skin appendages in a novel skin island rat model. J Chin Med Assoc 2019;82(8):635-42. DOI:10.1097/JCMA.0000000000000134.
82. Duan M, Zhang Y, Zhang H, Meng Y, Qian M, Zhang G. Epidermal stem cell-derived exosomes promote skin regeneration by downregulating transforming growth factor-β1 in wound healing. Stem Cell Res Ther 2020;11:452. DOI:10.1186/s13287-020-01971-6.

83. Li J, Ma J, Zhang Q, Gong H, Gao D, Wang Y, *et al*. Spatially resolved proteomic map shows that extracellular matrix regulates epidermal growth. Nat Commun 2022;13(1):4012. DOI:10.1038/s41467-022-31659-9.

84. Chang M, Nguyen TT. Strategy for treatment of infected diabetic foot ulcers. Acc Chem Res 2021;54(5):1080-93. DOI:10.1021/acs.accounts.0c00864.

85. Geiger BC, Wang S, Padera Jr RF, Grodzinsky AJ, Hammond PT. Cartilage-penetrating nanocarriers improve delivery and efficacy of growth factor treatment of osteoarthritis. Sci Transl Med 2018;10(469):eaat8800. DOI:10.1126/scitranslmed.aat8800.

86. Sowa Y, Kishida T, Tomita K, Adachi T, Numajiri T, Mazda O. Involvement of PDGF-BB and IGF-1 in activation of human Schwann cells by platelet-rich plasma. Plast Reconstr Surg 2019;144(6):1025e-36e. DOI:10.1097/PRS.0000000000006266.

87. You D, Nam M. Effects of human epidermal growth factor gene-transfected mesenchymal stem cells on fibroblast migration and proliferation. Cell Prolif 2013;46(4):408-15. DOI:10.1111/cpr.12042.

88. Li D, Wu N. Mechanism and application of exosomes in the wound healing process in diabetes mellitus. Diabetes Res Clin Pract 2022;187:109882. DOI:10.1016/j.diabres.2022.109882.

89. Hesketh M, Sahin KB, West ZE, Murray RZ. Macrophage phenotypes regulate scar formation and chronic wound healing. Int J Mol Sci 2017;18(7):1545. DOI:10.3390/ijms18071545.

90. Yang J, Liu X, Wang W, Chen Y, Liu J, Zhang Z, *et al*. Bioelectric fields coordinate wound contraction and re-epithelialization process to accelerate wound healing via promoting myofibroblast transformation. Bioelectrochemistry 2022;148:108247. DOI:10.1016/j.bioelechem.2022.108247.

91. Tan WS, Arulselvan P, Ng S-F, Mat Taib CN, Sarian MN, Fakurazi S. Improvement of diabetic wound healing by topical application of Vicenin-2 hydrocolloid film on Sprague Dawley rats. BMC Complement Altern Med 2019;19(1):20. DOI:10.1186/s12906-018-2427-y.

92. Farghali HA, AbdElKader NA, Khattab MS, AbuBakr HO. Evaluation of subcutaneous infiltration of autologous platelet-rich plasma on skin-wound healing in dogs. Biosci Rep 2017;37(2):BSR20160503. DOI:10.1042/BSR20160503.

93. Hsu H-H, Wang AYL, Loh CYY, Pai AA, Kao H-K. Therapeutic potential of exosomes derived from diabetic adipose stem cells in cutaneous wound healing of db/db mice. Pharmaceutics 2022;14(6):1206. DOI:10.3390/pharmaceutics14061206.

94. Jiang M, Jiang X, Li H, Zhang C, Zhang Z, Wu C, *et al*. The role of mesenchymal stem cell-derived EVs in diabetic wound healing. Front Immunol 2023;14:1136098. DOI:10.3389/fimmu.2023.1136098.

95. Lei X, Cheng L, Yang Y, Pang M, Dong Y, Zhu X, *et al*. Co-administration of platelet-rich plasma and small intestinal submucosa is more beneficial than their individual use in promoting acute skin wound healing. Burns Trauma 2021;9:tkab033. DOI:10.1093/burnst/tkab033.

96. Rodero MP, Hodgson SS, Hollier B, Combadiere C, Khosrotehrani K. Reduced Il17a expression distinguishes a Ly6cloMHCIIhi macrophage population promoting wound healing. J Invest Dermatol 2013;133(3):783-92. DOI:10.1038/jid.2012.368.

97. Novak ML, Koh TJ. Macrophage phenotypes during tissue repair. J Leukoc Biol 2013;93(6):875-81. DOI:10.1189/jlb.1012512.

98. Vasina EM, Cauwenberghs S, Staudt M, Feijge MA, Weber C, Koenen RR, *et al*. Aging-and activation-induced platelet microparticles suppress apoptosis in monocytic cells and differentially signal to proinflammatory mediator release. Am J Blood Res 2013;3(2):107-23. PMID: 23675563; PMCID: PMC3649808.

99. Lv S-S, Liu G, Wang J-P, Wang W-W, Cheng J, Sun A-L, *et al*. Mesenchymal stem cells transplantation ameliorates glomerular injury in streptozotocin-induced diabetic nephropathy in rats via inhibiting macrophage infiltration. Int Immunopharmacol 2013;17(2):275-82. DOI:10.1016/j.intimp.2013.05.031.

الملخص العربى

الإمكانات العلاجية للبلازما الغنية بالصفائح الدموية و/ أو الخلايا الجذعية الوسيطة على التئام جروح داء السكرى: دراسة نسيجية ومناعية كيميائية

بدرية حسن سعد[١]، ايمان العزب بحيرى[١]، نانسى محمد السقيلى[١]، سمر صبحى ابراهيم[٢]، دينا محمد رستم[٣]، رشا ربيع سالم[١]

[١]قسم التشريح الأدمي وعلم الأجنة، [٢]مركز التميز للأبحاث في الطب التجديدى وتطبيقاته،

[٣]قسم الهستولوجيا وبيولوجيا الخلية ـ كلية الطب ـ جامعة الاسكندرية

الخلفية: الجروح غير القابلة للالتئام هى مشكلة صحة عامة مهمة واستنزافا ماليا كبيرا على نظام الرعاية الصحية. لقد تم اثبات نجاح البلازما الغنية بالصفائح الدموية فى تجارب عديدة وذلك أنها غنية بالعديد من السيتوكينات والبروتينات الهامة لالتئام الجروح. العوامل الغذائية التى تتحكم فى الالتهاب واعادة التشكيل تفرز بواسطة الخلايا الجزعية الوسيطة المشتقة من نخاع العظم، وبالتالى يمكن ان تساعد فى التئام الجروح.

الهدف: كان الهدف من هذه الدراسة هو تقييم التأثيرات المورفولوجية والنسيجية والمناعية للبلازما الغنية بالصفائح الدموية و/او الخلايا الجزعية الوسيطة المشتقة من نخاع العظم على التئام الجروح الجلدية في الجرذان المصابة بداء السكري.

المواد وطرق البحث: مائة ذكرًا من الجرذان البيضاء السليمة؛ تم استخدام عشرة جرذان كمتبرعين بالخلايا الجذعية الوسيطة، والبلازما الغنية بالصفائح الدموية.تم استخدام ثماني عشر جرذا كمجموعة ضابطة سلبية(أ). تم تقسيم اثنين وسبعين جرذًا(ب) إلى ٤ مجموعات، كل منها ١٨ جرذًا بعد الإصابة بداء السكري بواسطة عقار الستربتوزوتوسين وعمل جروح جلدية؛ المجموعة الأولى: المجموعة الضابطةالايجابية، المجموعة الثانية : تلقت جرعة واحدة من حقن البلازما الغنية بالصفائح الدموية في الجرح، المجموعة الثالثة: تلقت جرعة واحدة من حقن الخلايا الجزعية الوسيطة المشتقة من نخاع العظم في الجرح، المجموعة الرابعة: البلازما الغنية بالصفائح الدموية بالإضافة إلى الخلايا الجزعية الوسيطة المشتقة من نخاع العظم . تم فحص الجروح الجلدية وتصويرها كل يومين للدراسة المورفولوجية. تم إجراء عمليات جراحية على ستة جرذان من كل مجموعة في اليوم السابع والرابع عشر والثلاثين من الدراسة لإجراء الدراسات النسيجية والكيميائية المناعية.

النتائج: أفضل نتائج الشفاء شوهدت في المجموعة الرابعة فيما يتعلق بالنتائج المورفولوجية والنسيجية والمناعية مع وجود فرق ذو دلالة إحصائية بين المجموعة الرابعة ومجموعات الدراسة التجريبية الأخرى. أظهرت المجموعة الثالثة نتائج شفاء أفضل من المجموعة الثانية والتي أظهرت نتائج أفضل من المجموعة الأولى.

الاستنتاج: هناك تأثير تآزري لكل من الخلايا الجزعية الوسيطة المشتقة من نخاع العظم والبلازما الغنية بالصفائح الدموية مجتمعين على شفاء الجلد من الجروح في الجرذان المصابة بداء السكري الناجم عن الاستربتوزوتوسين وهو ذو فائدة أكبر من استخدام أي منهما بمفرده.